BB293

Florida A & M University - Florida State University
College of Engineering

Department of Civil Engineering

EFFECTS OF BOUNDARY CONDITIONS ON BRIDGE PERFORMANCE

WP Item No. 0510843

A
Final Report
Submitted to the
Florida Department of Transportation

By
Nur Yazdani, Ph.D., P.E.
and
Tanya Green

March, 2000

Technical Report Documentation Page

1. Report No.	2. Government Accession No.	3. Recipient's Catalog No.
WP Item No. 0510843		

4. Title and Subtitle	5. Report Due
Effects of Boundary Conditions on Bridge Performance	
	6. Performing Organization Code: 6120-540-39
	8. Performing Organization Report No.: 6120-540-39
7. Author's: Nur Yazdani, Ph.D., P.E. and Tanya Green	
9. Performing Organization Name and Address: FAMU-FSU College of Engineering, 2525 Pottsdamer St, Tallahassee, FL 32310	10. Work Unit No. (TRAIS)
	11. Contract or Grant No.: BB-293, 99700-3867-119
	13. Type of Report and Period Covered: 9/8/97 – 11/1/99
12. Sponsoring Agency Name and Address: Florida Department of Transportation, 605 Suwannee Street, Tallahassee, FL 32399-0450	14. Sponsoring Agency Code

15. Supplementary Notes

Prepared in cooperation with the US department of Transportation and Federal Highway Administration

16. Abstract

Reinforced elastomeric bearing pads generally support precast concrete bridge girders. The condition of these bearing pads and the pad-bridge interface define the support boundary conditions of the bridge superstructure. The interface between bearing pads and bridge girders affect the performance of the superstructure and the substructure. The pads are designed to carry vertical loads, and to accommodate horizontal movements of the bridge girders. The objectives of this study were to determine the effects of various parameters on the bridge superstructure performance and to compare the girder performance with simple support conditions corresponding to the current FDOT design. A parametric study on the interaction of the support boundary conditions and bridge girders was performed in this study. Some of the parameters included; the skewness of the bridge, the presence of intermediate diaphragms, and the temperature effects on the bridge superstructure. A finite element model of a bridge superstructure containing Florida Bulb Tee 78 girders was created using ANSYS software. This model was subjected to an HL93 truck load as pertaining to LRFD AASHTO specifications. The results indicate that pads with higher bearing stiffness are beneficial to bridges with higher skew angles. Intermediate diaphragms have the positive effect of reducing the overall midpoint deflections and maximum stresses for the bridge system. However, the reductions in deflections and stresses are smaller for increasing skew angles.

17. Key Words	18. Distribution Statement
Bearing Pads, Bearing Stiffness, Skewness, Bridge Performance,	No restriction. This report is available to the public through the National Technical Information Service, Springfield VA 22161

19. Security Classif. (of this report)	20. Security Classif. (of this page)	21. No. of Pages	22. Price
Unclassified	Unclassified		

Form DOT F 1700.7 (8-72)

EFFECTS OF BOUNDARY CONDITIONS ON BRIDGE PERFORMANCE

By

Nur Yazdani, Ph. D., P.E.
and
Tanya Green

Research Project No. WPI 0510843

A Final Report Submitted to
The Florida Department of Transportation

Department of Civil Engineering
FAMU-FSU College of Engineering
Tallahassee, Florida 32310

March, 2000

The opinions, findings and conclusion expressed in this publication are those of the authors and not necessarily those of the Department of Transportation or the U.S. Department of Transportation.

Prepared in cooperation with the State of Florida Department of Transportation and the U.S. Department of Transportation.

TABLE OF CONTENTS

	Page
List of Tables	iv
List of Figures	vi
Chapters 1: Introduction	1
1.1 Problem Statement	1
1.2 Objectives	2
Chapter 2: Literature Review	3
2.1 Bearing Pads	3
2.2 Slab Bridges	5
2.3 Temperature Effects	6
2.4 Skewed Bridges	7
Chapter 3: Properties of Bearings Pads	10
3.1 Introduction to Bearing Pads	10
3.2 AASHTO Specifications	15
3.2.1 Classification	15
3.2.2 Material Properties	16
Chapter 4: Finite Element Modeling	19
4.1 Girder Selected for Study	19
4.2 Types of Elements	19
4.2.1 Concrete Element	19
4.2.2 Spring Element	20
4.3 Development of Model	22

4.3.1 Loading 23

4.4 Straight Bridge Model 23

4.4.1 End Diaphragms 25

4.4.2 Spring Placement 25

4.5 Skewed Bridge 28

4.5.1 Intermediate Diaphragms 28

4.6 Temperature 28

Chapter 5: Results and Discussion 30

5.1 Parametric Matrix 30

5.2 Effect of Skewness and Bearing Stiffness 32

5.2.1 Discussion 37

5.3 Effect of Intermediate Diaphragms 39

5.3.1 Discussion 45

5.4 Effect of Temperature Changes 46

5.4.1 Discussion 52

6. Conclusions and Recommendations 54

Bibliography 56

LIST OF TABLES

No.		Page
4.1	Material Properties	23
4.2	Location of Truck Loads	26
4.3	Spring Stiffness Values of Florida Bulb Tee Girder Model	27
5.1	Effect of Skewness and Bearing Stiffness	30
5.2	Effect of Intermediate Diaphragms	31
5.3	Effect of Temperature Change (Negative Differential)	31
5.4	Effect of Temperature Change (Positive Differential)	31
5.5	Combined Effect of Skewness and Bearing Stiffness (Maximum Deflection, mm)	32
5.6	Percent Difference in Maximum Deflection Due to Skewness and Bearing Stiffness (All Values Compared to Straight Bridge)	32
5.7	Combined Effect of Skewness and Bearing Stiffness (Maximum Tensile Stresses, MPa)	33
5.8	Percent Difference in Maximum Tensile Stresses Due to Skewness and Bearing Stiffness (All Values Compared to Straight Bridge)	33
5.9	Combined Effect of Skewness and Bearing Stiffness (Total Vertical Reaction, kN)	33
5.10	Vertical Reactions Across Bridge (kN)	34
5.11	Combined Effect of Skewness and Bearing Stiffness (Total Horizontal Reactions, Left Support, kN)	34
5.12	Combined Effect of Skewness and Bearing Stiffness (Total Horizontal Reactions, Right Support, kN)	35
5.13	Effect of Intermediate Diaphragms (Maximum Deflection ,mm)	39
5.14	Percent Difference in Maximum Deflection Due to Skewness and Bearing Stiffness (All Values Compared to Straight Bridge)	39

5.15 Effect of Intermediate Diaphragms (Maximum Tensile Stresses, MPa) 40

5.16 Percent Difference in Maximum Tensile Stresses Due to Skewness and Bearing Stiffness (All Values Compared to Straight Bridge) 40

5.17 Effect of Intermediate Diaphragms (Total Vertical Reaction, kN) 40

5.18 Vertical Reactions Across Bridge (kN) 41

5.19 Effect of Intermediate Diaphragms (Total Horizontal Reaction, Left Support, kN) 41

5.20 Effect of Intermediate Diaphragms (Total Horizontal Reaction, Right Support, kN) 42

5.21 Effect of Temperature Change (Positive Temperature Differential, Maximum Deflection, mm) 47

5.22 Effect of Temperature Change (Negative Temperature Differential, Maximum Deflection ,mm) 47

5.23 Effect of Temperature Change (Positive Temperature Differential, Maximum Tensile Stresses, GPa) 47

5.24 Effect of Temperature Change (Negative Temperature Differential, Maximum Tensile Stresses ,GPa) 48

LIST OF FIGURES

No.		Page
3.1	Plain Bearing Pad	12
3.2	Laminated Bearing Pad	12
3.3	Laminated Bearing Pad, Isometric View	12
3.4	Vertical Dead and Live Load Forces on Girder and Bearing Pad	13
3.5	Horizontal Forces on Girder and Bearing Pad	13
3.6	Rotational Forces on Girder and Bearing Pad	14
3.7	Combination of Forces and Girder and Bearing Pad	14
4.1	Plan View of I-95 Bridge	21
4.2	Dimensions of Type V Bearing Pad	22
4.3	Cross-Sectional Area of Florida Bulb Tee 78 Girder	24
4.4	Extruded Volume of Girder	24
4.5	HL93 Design Truck Spacing (AASHTO)	26
4.6	Outline of Diaphragm	26
4.7	Tributary Area for Placement of Spring Elements	27
4.8	Tributary Area and Placement for Skewed Spring Elements	29
4.9	Typical View of the Intermediate Diaphragms	29
5.1	Maximum Midpoint Deflections for Various Bearing Stiffness and Skew Angles (End Diaphragms Only)	35
5.2	Maximum Tensile Stresses for Various Bearing Stiffness and Skew Angles (End Diaphragms Only)	36
5.3	Comparison of Vertical Reactions Across Bridge Girders for 15° Skew and G = 0.655 GPa (End Diaphragms Only)	36

5.4 Comparison of Vertical Reactions Across Bridge Girders for 60° Skew and G = 0.655 GPa (End Diaphragms Only) 37

5.5 Maximum Deflections for Various Bearing Stiffness and Skew Angles (End and Intermediate Diaphragms) 42

5.6 Comparison of Maximum Deflection for Various Skew Angles with Intermediate and End Diaphragms for G = 0.655 and 6.895 Gpa 43

5.7 Maximum Tensile Stresses for Various Bearing Stiffness and Skew Angles (Intermediate Diaphragms) 43

5.8 Comparison of Maximum Tensile Stresses for Various Skew Angles with Intermediate Diaphragms for G = 0.655 and 6.895 Gpa 44

5.9 Comparison of Vertical Reactions Across Bridge Girder for 15° Skew (End and Intermediate Diaphragms) 44

5.10 Comparison of Vertical Reactions Across Bridge Girder for 60° Skew (End and Intermediate Diaphragms) 45

5.11 Maximum Midpoint Deflections for Various Bearing Stiffness and Skew Angles for Positive Temperature Differential (End Diaphragms Only) 48

5.12 Maximum Midpoint Deflections for Various Bearing Stiffness and Skew Angles for Negative Temperature Differential (End Diaphragms Only) 49

5.13 Comparison of Maximum Deflection for 15° Skew Angle with Temperature Differentials for G = 0.655 GPa (End Diaphragms Only 49

5.14 Comparison of Maximum Deflection for 60° Skew Angle with Temperature Differentials for G = 0.655 GPa (End Diaphragms Only) 50

5.15 Maximum Tensile Stresses for Various Bearing Stiffness and Skew Angles for Positive Temperature Differential (End Diaphragms Only) 50

5.16 Maximum Tensile Stresses for Various Bearing Stiffness and Skew Angles for Negative Temperature Differential (End Diaphragms Only) 51

5.17 Comparison of Maximum Tensile Stresses for Various Skew Angles with Temperature Differentials for G = 0.655 GPa (End Diaphragms Only) 51

5.18 Comparison of Maximum Tensile Stresses for Various Skew Angles with Temperature Differentials for G = 6.895 GPa (End Diaphragms Only) 52

CHAPTER 1

INTRODUCTION

1.1 Problem Statement

Reinforced elastomeric bearing pads generally support precast concrete bridge girders. The condition of these bearing pads and the pad-bridge interface define the support boundary conditions of the bridge superstructure. The interface between bearing pads and bridge girders affect the performance of the superstructure and the substructure. The pads are designed to carry vertical loads, and to accomodate horizontal movements of the bridge girders. The elastomeric bearing pads are designed to deflect horizontally under shearing-type forces. These girder movements can be caused by several factors including temperature and longitudinal thrust. In addition to the horizontal movement, the bearing pads maintain a rotational stiffness to accommodate the end rotations of the girders under load. In the design of the bridge girders, simple support conditions are normally assumed with no horizontal bearing restraint forces imparted on the girders. Due to the nature of the elastomeric material and its resistance to shearing, horizontal forces are present under service load conditions as the horizontal movement of the bridge girders apply load and deform the bearing pad. The effects of these forces on the performance of the bridge girders are unknown. The effect of some other bridge parameters in conjunction with the bearing pad effect is also not known. It is possible that forces existing as a result of the boundary conditions could improve or alter the performance of bridge girders. The LRFD AASHTO specifications for highway bridges do not address the resistance effect of bearing pad construction in its design specification for bridge girders. A parametric study on the interaction of the support boundary conditions and bridge girders was performed in this project.

The performance of bridge superstructures under various combinations of parameters was explored in this study. Parameters affecting the superstructure performance and included in this study are:

- Type of bridge girder
- Girder length and spacing
- Bearing pad type
- Static loading
- Skewness of bridge
- Presence of intermediate diaphragms
- Temperature effects

1.2 Objectives

The objectives of this study were:

1) To determine the material and stiffness properties of typical elastomeric bearing pads
2) To utilize a commercial finite element analysis (FEA) program to model the Florida Bulb Tee 78 girder, and analyze the loading response and girder performance under the established boundary conditions.
3) To determine the effects of the various parameters on the bridge superstructure performance
4) To compare the girder performance with simple support conditions corresponding to the current FDOT design.
5) To provide recommendations regarding the effect of the boundary conditions on the performance of the girders.

CHAPTER 2

LITERATURE REVIEW

2.1 Bearing Pads

Researchers at the University of Oklahoma tested several materials in an effort to determine the best material for application in bridge bearing pads (Aldridge, 1968). In this experiment, five elastomeric bridge bearing materials were analyzed: neoprene, butyl, EPT, and chlorobutyl. The scope of the test involved the use of bonded and unbonded pads that were tested for various bridge applications. The bonded pads tested were laminated and conformed to ASTM standards and were attached to thin steel shims. The tests included compression-deflection, static creep, and repetitive reversed shear tests. These tests indicated that all materials tested were very similar for compression-deflection. The static creep tests indicate that the bonded pads show a significant advantage over the unbonded pads. This research also indicated that laminated pads have better load-deformation behavior than solid pads, and that butyl, neoprene, EPT, and chlorobutyl all demonstrated acceptable load-deflection and abrasion characteristics.

In 1963, the findings of researchers at the University of Rhode Island and Enjay Laboratories were presented at the 42nd annual meeting of the Highway Research Board. (Clark, 1963) The materials selected consisted of 6 x 12 x 1 in molded pads of butyl, chlorobutyl, and neoprene. The neoprene and butyl pads used satisfied the American Association of State Highway Officials (AASHO) limits for hardness and shape factors. The chlorobutyl pad was the only pad that exhibited properties below the tensile strength specifications. The pads were subjected to compressive and shear load deformation tests at room temperature of $23^{\circ} \pm 4^{\circ}$ C and

at low temperature of $-7 \pm 4^{\circ}$ C, repeated after an accelerated aging process was applied to the materials. This aging process was designed to simulate many years of normal temperature exposure. Other tests that were performed included simulated fatigue tests, and water absorption tests. The results of the tests indicated that both butyl and neoprene pads were nearly identical in load deflection for the compressive and shear load tests, while the chlorubutyl bearing showed a greater deflection. The fatigue tests indicated consistent results for all bearings tested. The water absorption tests indicate that the butyl showed no increase in volume, while the chlorobutyl and neoprene showed a 1½ percent, and 4½ percent increase in volume, respectively. The low temperature evaluations indicated that neoprene was substantially stiffer than the other bearing materials. At lower temperatures, accurate horizontal deflection results could not be determined for the neoprene pads due to slippage during testing. Brielmaier also showed that the effectiveness of neoprene could be reduced over a long period of low temperature exposure. (Brielmaier, 1964)

The California Division of Highways conducted laboratory and field performance tests in an effort to determine the best design for elastomeric bridge bearing pads (Nordlin 1972). Tests were performed on bonded and unbonded solid elastomeric neoprene bearing pads and on different composites such as steel, Dacron, and nylon between the interfaces of the horizontal layers. The results indicate that the laminates should not exceed 12 mm thickness for any of the tested materials. The fabric-laminated pads were shown to perform as well as steel-laminated pads, with greater convenience and economy of construction (Nordlin 1972).

A recent study on the effects of bearings pads on precast concrete girders was undertaken at the FAMU-FSU College of Engineering (Eddy 1997). A finite element program, ANSYS, was used to model several bridge types. The researcher modeled AASHTO Type III and V girders

with applied static AASHTO truck loads. Spring elements were used to simulate the bearing pads at the ends of each girder. The results of this study indicate that ignoring the effects of the bearing pads would result in a more conservative bridge design. It was concluded that the bearing pads were serving the overall purpose adequately, which is to provide minimum horizontal restraint forces to the girder while allowing horizontal movement.

2.2 Slab Bridges

Tests performed on a large number of bridges in Ontario between 1973 and 1988 have shown that slab-on-girder bridges are significantly stiffer in flexure than had been predicted by analysis (Bakht 1988). This study concluded that slab-on-girder bridges are stiffer because of horizontal restraint provided by the end restraints. The researchers presented a case study in support of the contention that observed girder stresses in actual slab-on-girder bridges under tests loads were much smaller than expected, and that the sum of girder moments computed from measured girder strains was significantly smaller than the corresponding moment obtained by treating the whole bridge as a simply supported beam. Bakht was able to conclude that the bearing restraint forces can cause a reduction in the girder live load moments by a minimum of 15% and a maximum of 26%.

Bakht and Jaeger conducted an ultimate load test on a slab-on-girder bridge in the city of London, Ontario, Canada (Bakht 1992). The test was conducted on the Stoney Creek Bridge which is a straight, short-span, two-lane bridge having a concrete deck slab and six rolled steel girders that were simply supported on concrete abutments. The test was conducted by loading the bridge with concrete blocks until failure occurred. It was concluded based on the strain readings that the load at which an individual girder was not able to sustain any additional load is significantly higher than the point at which the girder experiences first yield. It was also

concluded that the bridge as a whole was able to sustain loads long after the individual girder limitations had been reached. It was concluded that the bearing restraint forces reduced the applied moments by a minimum of 11%, and that neglecting the bearing restraint forces in the calculation of girder moments may lead to a significant overestimation of girder moments.

2.3 Temperature Effects

NCHRP funded a study concerning the low temperature behavior of elastomeric bridge bearings (Feller, et al 1989). The objective was to provide a comprehensive description of research related to low temperature stiffening of elastomers used in bridge bearings. The existing research had concluded that elastomers my be many times stiffer at low temperatures than at room temperature resulting in forces in the bridge that were much larger than anticipated in the design. Crystallization or instantaneous thermal stiffening may cause this stiffening effect. This is dependent on time and temperature, and is very sensitive to the elastomer compound, according to this research. Elastomers could also reach a brittle state known as the glass transition at very low temperatures (Feller, et al 1989). Low temperatures my cause dramatic increases in the stiffness of elastomeric bearings and the increased stiffness may result in significant increases in the forces transmitted by the bearing to the substructure. The research indicated that neoprene generally experience greater low temperature stiffness than comparable natural rubber compounds. According to this research, elastomer may experience stiffness that is more than 50 times their room temperature stiffness, at $-50^{\circ}C$ or lower for all compounds examined in their research. It was also determined that elastomers recover their room temperature stiffness shortly after the temperature is raised above a critical value of approximately $+10^{\circ}C$ rather than the $15^{\circ}C$ above crystallization as suggested in previous research.

Moorty and Roeder conducted a study based on the temperature dependent bridge movements. The focus of this research was to analyze the response of several bridges exposed to thermal environmental conditions. Analytical methods were developed to obtain temperature distributions and the maximum bridge temperature ranges of straight, skewed and curved bridges (Moorty and Roeder 1992).

It was concluded that the AASHTO method for predicting thermal movements was adequate for straight orthogonal bridges, but a more refined analysis was required for skewed and curved bridges. The transverse movements and stresses were found to increase with increasing skew angle and width of bridge. This increase may cause skew and curved bridges to have frequent maintenance to ensure satisfactory performance of the bearings and expansion joints. The researchers state that integral construction is clearly a viable method for accommodating thermal movements in some bridges, yet it is not a solution to all thermal movement. Integral construction would restrain the movement through the stiffness of the substructure, foundation, and backfill, which increases the forces within the bridge. These forces must be accommodated in the design or they may lead to unexpected damage (Moorty and Roeder 1992).

2.4 Skewed Bridges

Khaleel and Itani conducted a study on the live-load moments for continuous skew bridges (Khaleel and Itani 1990). This study presented a method for determining moments in continous normal and skew slab and girder bridges due to live loads. The study used the finite element method to analyze 112 continuous bridges. Each bridge analyzed had five pretensioned I-girders with varying spans between 24.4 and 36.6 m, and are spaced between 1.8 and 2.7 m. The angle of skew was varied between 0 and 60°. They performed a convergence study on a

control bridge to ensure reliable results. The results of the parametric study indicated that a reduction in the girder moment was noted as the skew angle increases. For an angle of skew less than 30°, the reduction in the interior girder moment was stated to be negligible, while the effect of skew angles increased when greater than 45°. It was also noted that when the skew angles exceed 45° the exterior girder moments are sensitive to change. It was concluded that for bridges with smaller stiffness ratios between girder and slab and long spans, the exterior girders would control design. It was determined that larger skew angles yield significantly smaller design moments for both interior and exterior girders.

Bishara conducted a study on multisteel beam composite bridges of medium span length to determine wheel load distribution factors on simply supported skew I-beam composite bridges (Bishara 1993). The objective of the study was to suggest wheel load distribution factors which consider the effects of bridge skew angle, span length, bridge total width, number of loaded traffic lanes, spacing and stiffness of intermediate cross frames, and restraining forces at the bearings. The analysis of the results indicate that the live load maximum bending moments in girders of skew bridges are generally lower than those in right bridges of the same span and deck width. It was determined that the larger the skew angle, the smaller the bending moment. The maximum interior girder's bending moment caused by skew was found to be around 5% for a skew angle of 30°, however the reduction can become as large as 28% for a skew angle of 60°. It was also noted that the moment reduction is relatively smaller in exterior girders. The maximum exterior girders' bending moment has a 10% increase in skew angles of 20°, and 5% for skew angles of 40°, however for 60° skew bridges, this behavior was found to be reversed with a decrease in the distribution factor of 25% from a right bridge.

Arokiasamy and Bell at the Florida Atlantic University conducted research based on the load distribution on highway bridges based on field test data. This primary aim of this study was to investigate the wheel load distribution of different bridge types –solid slab bridges and slab-on-girder bridges with varying skew angles and multiple continuous span lengths. The parameters studied included skew angle, girder spacing, span length, slab thickness, and number of traffic lanes. The response of the continuous bridges was studied by modeling several continuous bridge types using finite element method. The wheel load distribution factors from the analysis were compared with the field test data taken from the a previous paper conducted by the principal investigator (Arockiasamy 1994), on "Load Distribution on Highway Bridges Based on Field Test Data - Phase I". The objective of the current research was to determine the load distribution factors for slab-on-girder bridges, skew bridges, and continuous bridges. The overall results of this study for all bridge types indicate that the AASHTO and LRFD codes for load distribution factors are conservative for design. The analysis performed indicates that this is adequate for design considerations, however for ratings of existing bridges for load capacity, more accurate methods should be used.

CHAPTER 3

PROPERTIES OF BEARING PADS

3.1 Introduction to Bearing Pads

Neoprene bearing pads provide an economical and efficient method for supporting precast concrete bridge girders. These elastomeric bearing pads are molded or cut from a molded sheet of high-grade, neoprene synthetic rubber compound. The pads are composed of multiple laminate layers of elastomeric material separated by steel reinforcing, which are cast as a unit in a mold under pressure and heat, creating a vulcanized unit. The elastomeric material has the ability, under certain conditions, to undergo large deformations and recover almost completely and instantaneously upon release of the deforming forces (Eddy 1997). They are placed between the girder and support to allow longitudinal bridge movements due to thermal expansion and contraction, concrete shrinkage and creep, and traffic loads. Neoprene pads permit a smooth and uniform transfer of load from the girder to the substructure and allow girder rotation at the bearing due to deflection of the girder under load.

Elastomeric bearing pads have been in use since the mid to late 1950's, and neoprene synthetic rubber bearing pads have been used since 1957. Bearing pads come in many types that can be classified into four categories: plain pads, randomly-oriented fiber-reinforced pads, layered fiber reinforced bearings, and steel-reinforced bearing pads. The Florida Department of Transportation (FDOT) began using steel-laminated bearing pads in the late 1960's. The FDOT specifies that all pads supporting AASHTO and Florida Bulb Tee precast concrete girders must utilize steel-laminated neoprene pads (FDOT 1999). Figures 3.1 and 3.2 show the two categories

of bearing pads, plain elastomeric pads and laminated steel-reinforced bearing pads. An isometric view of a steel-reinforced laminated bearing pad is presented in Fig. 3.3.

Polychloroprene (CR), also known as neoprene, is manufactured from a raw polymer in chip form. It is compounded into a crosslinked thermoset elastomer through the addition of carbon black, plasticizers and curatives. The vulcanization process occurs at a temperature between 140 – 200° C (284 – 392° F). This temperature causes a chemical reaction to occur which crosslinks, or cures, the compound. The steel laminates are combined with the elastomer and the vulcanization process occurs in a mold of the finished bearing pads. (Eddy 1997)

Steel-laminated elastomeric reinforced bearing pads are designed to support vertical compressive loads and to allow horizontal movement of the bridge girder due to thermal expansion and contraction, traffic loads, elastic shortening, girder end rotations and concrete time-dependent changes (Eddy 1997). The neoprene layers between the steel laminates allow horizontal movement of the top and bottom bearing surfaces relative to one another. This has been shown not to affect the pads ability to deflect under shear forces (Roeder and Stanton 1987). A properly designed and fabricated steel-reinforced bearing can sustain large compressive stresses and permit shear deformations. Several possible girder movements and resulting pad reactions are illustrated in Figs. 3.4 through 3.7.

Research has shown that low temperatures have an effect on elastomeric bridge bearings that could lead to increased shear forces, and a significant increase in the allowable load capacity of some bridge bearings (Feller, et al 1989). Crystallization or instantaneous thermal stiffening may cause this low temperature stiffening effect. This crystallization effect is time and temperature dependent and is responsive to the elastomeric compounds. Low temperatures may

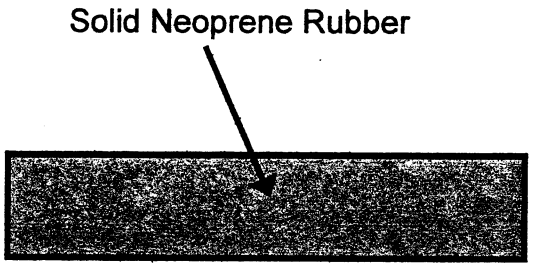

Figure 3.1: Plain Bearing Pad

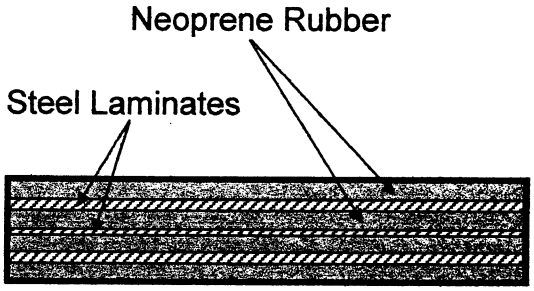

Figure 3.2: Laminated Bearing Pad

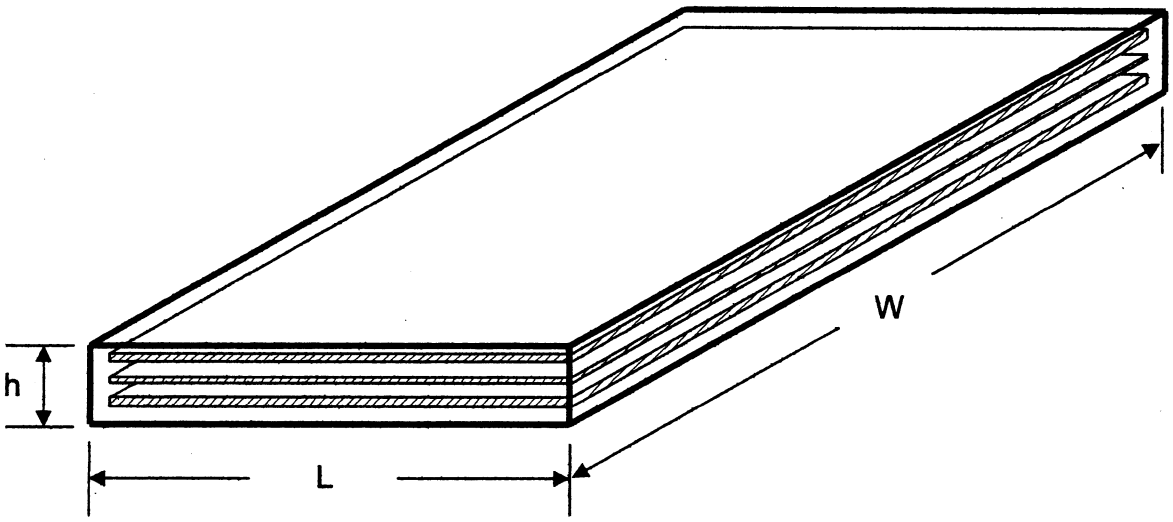

Figure 3.3: Laminated Bearing Pad, Isometric View

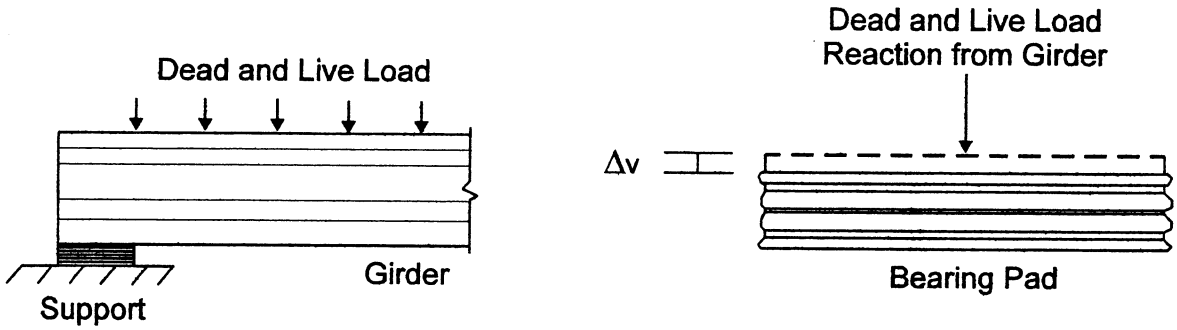

Figure 3.4: Vertical Dead and Live Load Forces on Girder and Bearing Pad

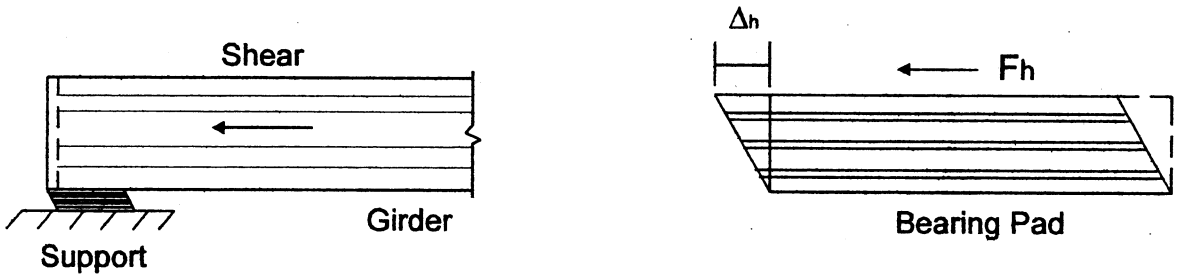

Figure 3.5: Horizontal Forces on Girder and Bearing Pad

Figure 3.6: Rotational Forces on Girder and Bearing Pad

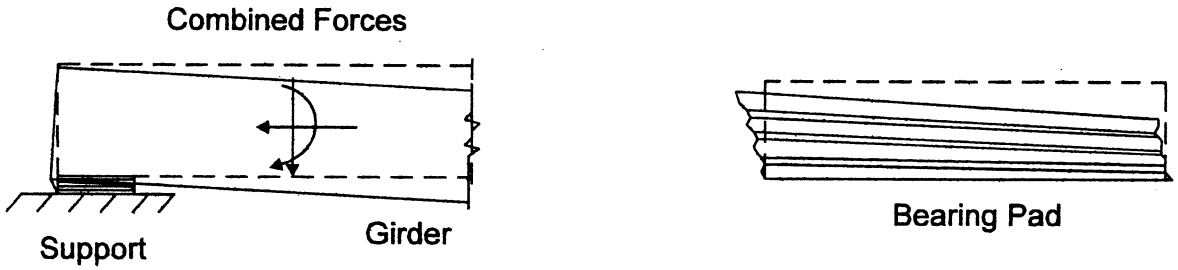

Figure 3.7: Combination of Forces on Girder and Bearing Pad (Eddy 1997)

also cause the elastomer to reach a brittle state known as the glass transition. A neoprene compound that is highly resistant to low temperature crystallization stiffness has been shown to experience a smaller stiffness increase than a natural rubber compound with poor crystallization resistance. (Feller, et al 1989)

3.2 AASHTO Specifications

3.2.1 Classification

Elastomeric materials are classified by their shear modulus and hardness. Shear modulus is considered to be the most important material property for design according to AASHTO. The shear modulus is the material property by which the mechanical properties of the bearing pad are determined. Bearing pads are typically specified by their hardness because of the ease of testing; however, this material property correlates loosely with the shear modulus. If the bearing pad is specified by its hardness, several estimates of shear modulus should be used to determine the most conservative design of the pad.

Hardness is the resistance of the elastomer to elastic indentation caused by a rigid indenter of prescribed size and shape (Gent 1992). Two types of hardness tests are commonly used: the International Rubber Hardness Tester which indicates the hardness in degrees (IRHD), and the Shore durometer hardness test which classifies the elastomer in order of increasing hardness according to the following classification: 000, 00, 0, A, B, C and D. Shore A is the most commonly used hardness in bearing pads and refers to the resistance to penetration of the rubber by a truncated cone indenter of precisely controlled dimensions (Gent 1992). AASHTO specifies that at 23° C (73° F), the elastomer used in bearing pads shall have a shear modulus of 0.60 to 1.2 MPa (90 to 170 psi) and a nominal hardness grade between 50 and 60 on the Shore A

scale (AASHTO 1998). FDOT specifies that the elastomer in all bearing pads have a grade 50-durometer hardness based on the Shore A scale. AASHTO specifies a range of shear modulus for an elastomer classified with a Shore A hardness of 50 to be of 0.66 to 0.90 MPa (95 to 130 psi). Previous research has shown that low temperatures may cause instantaneous stiffening and brittleness to be a factor in the hardness of the bearing pad elastomer. The shear modulus for a 50-durometer elastomer at –29° C has been determined to be approximately 1.4 MPa (Dupont 1983).

3.2.2 Material Properties

An elastomer is defined by its hardness, yet the shear modulus is its most important material property. The compressive stress-strain characteristics of any elastomer are controlled by its shear modulus and shape factor. The shape factor is defined as the ratio of the plain surface area loaded in compression of the elastomer to the area of the elastomer free to bulge. The shape factor is a dimensionless measure of the relative layer thickness (Stanton and Roeder 1987). For rectangular bearing pads, the shape factor is expressed by Eq. 3.1 (AASHTO 1998).

$$S = \frac{LW}{2h_{ri}(L+W)} \tag{3.1}$$

where:

S = shape factor of a layer of an elastomeric bearing

L = length of a rectangular elastomeric bearing (parallel to longitudinal bridge axis)

W = width of the bearing in the transverse direction

h_{ri} = thickness of a single layer of elastomeric bearing

Due to the non-linear load-deformation curve of an elastomeric bearing, The effective compressive modulus (E_c) is load dependent. One acceptable approximation for the effective modulus is given by Eq. 3.2 (AASHTO 1998).

$$E_c = 6GS^2 \text{ (SI)} \tag{3.2}$$

where: E_c = effective modulus of elastomeric bearing in compression

G = shear modulus of the elastomer

S = shape factor

Using the relationship between compressive modulus, stress and strain, the relationship between vertical displacement and compressive stress can be determined. The effective compressive stiffness can be defined as the amount of force required to compress the pad a unit distance. This compressive stiffness can be determined from Eq. 3.3:

$$K_c = \frac{F_c}{\delta} = \frac{A}{h_{rt}} E_c \tag{3.3}$$

where: K_c = effective compressive stiffness

A = loaded surface area

h_{rt} = total elastomer thickness of bearing

To accommodate horizontal movements of the bridge girders, the bearings are designed so that the total thickness of the elastomer in the bearing is equal to or greater than twice the allowable shear deflection. Restraint of movement due to the shear stiffness of the bearing pads

results in a moment in the structure. The horizontal restraining effects can then be calculated taking into account the shear stiffness of the bearings:

$$H = GA\frac{\Delta_h}{h_{rt}} \tag{3.4}$$

where:

H = largest horizontal force which can be transmitted (Design shear force on bearing)

A = plan area of elastomeric element or bearing (mm^2)

G = shear modulus of the elastomer

Δ_h = total horizontal movement of structure, measured from state at which bearing is undeformed

Rearranging Eq. 3.4 produces the horizontal stiffness provided by the bearings.

$$K_h = \frac{H}{\Delta_h} = \frac{GA}{h_{rt}} \tag{3.5}$$

where:

K_h = horizontal stiffness

CHAPTER 4

FINITE ELEMENT MODELING

4.1 Girder Selected for Study

The Florida Bulb Tee 78 was selected as the principal girder for the study because it is widely used by the FDOT. The computer model is based on a bridge in Duval County, Florida, spanning I-95 over the St. Johns River. The design plans were obtained from the Structures Design Office and the design firm of Howard, Needles, Tammen, & Bergendoff. The bridge was constructed as an expanded replacement for an older bridge. The new bridge was designed to support an eight-lane highway with a total length of 773 m. A typical plan view of the chosen bridge section is shown in Fig. 4.1.

ANSYS Version 5.5 was used to model the I-95 bridge chosen for this study. The first stage in developing the finite element model was to determine the necessary properties and geometry of the bridge. A typical cross section was chosen from the bridge, which consisted of a 45 m span supported by sixteen prestressed girders. Due to the limitations of ANSYS Version 5.5 University High Option, it was decided to model only eight girders utilizing the symmetry of the bridge.

4.2 Types of Elements

4.2.1 Concrete Element

The Florida Bulb Tee 78 bridge girder was modeled using the SOLID65 3-D reinforced concrete element from ANSYS. The element is used for 3-D concrete modeling with or without reinforcing bars. The element is capable of simulating concrete cracking and crushing, plastic

deformation, and creep. The rebars are capable of tension and compression, but are not able to carry shear. The concrete properties of the SOLID65 element were used as input for the preprocessor to represent the behavior of concrete with reinforcement. For elastic behavior, the element is considered as a linear elastic material. The behavior of the girders under the assumed load falls well within the elastic region of the members and the **SOLID65** concrete element is used herein as a linear element by removing the cracking and crushing properties of the assigned concrete material.

4.2.2 Spring Elements

The bearing pads were modeled using a COMBIN14 spring element from ANSYS. This element has longitudinal or torsional capability in one, two, or three-dimensional applications. The longitudinal spring-damper element is a uniaxial tension-compression element with up to three degrees of freedom at each node: translations in the nodal x, y, and z directions (ANSYS Elements Reference 1999). Two nodes, a spring constant (k) and damping coefficients, define this element. The damping capability is not used for static or undamped nodal analysis. For the purpose of this analysis, the spring constants (k) for compressive and horizontal movements were specified through AASHTO values. The spring elements were distributed over the bearing area for each girder. The type of bearing pad depends on the type of girder being supported. Type V bearing pads are to be used for Florida Bulb Tee girders. (FDOT 1999) The dimensions of the bearing pad are 254 by 610 mm, as shown in Fig. 4.2.

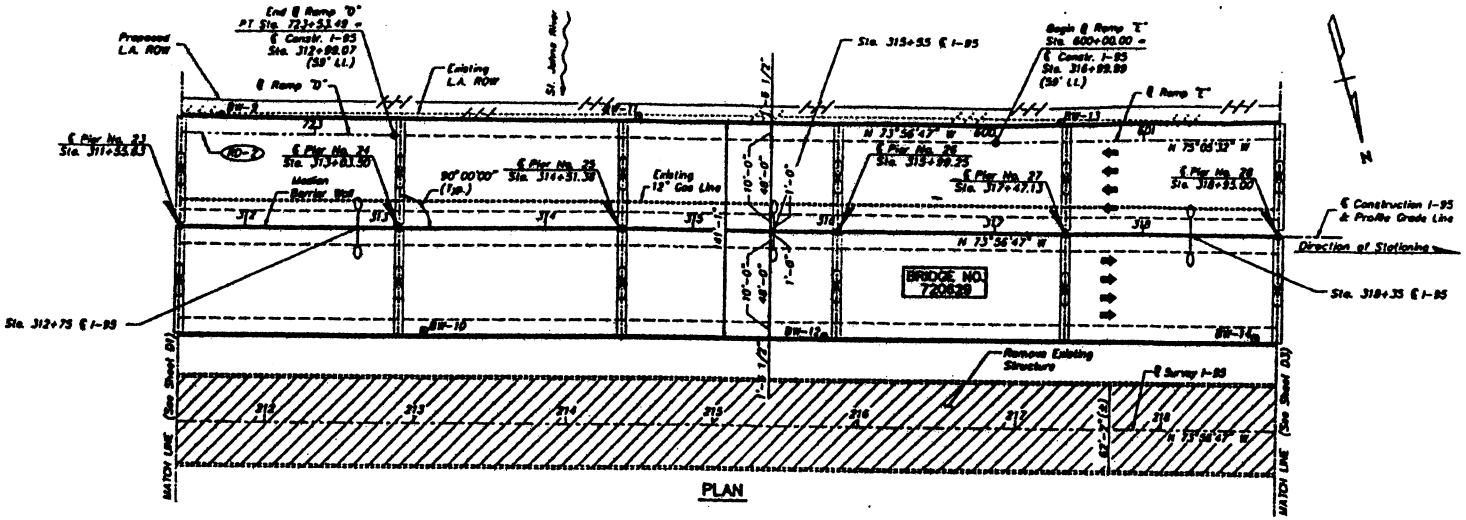

Figure 4.1 Plan View of I-95 Bridge

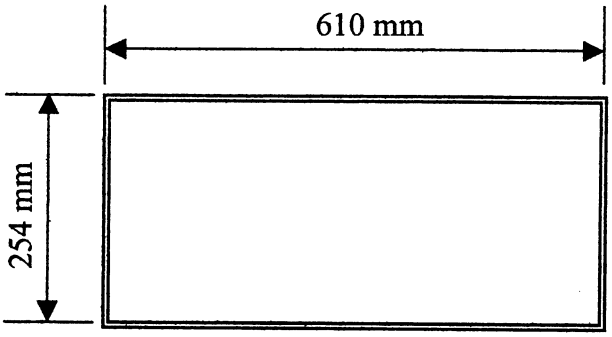

Figure 4.2 Dimensions of Type V Bearing Pad

4.3 Development of Model

The first step in the development of the model was the determination of the concrete properties. The input parameters for the FE analysis include Young's modulus of elasticity and the poisson's ratio. Equation 4.1 was used for Young's modulus of elasticity for concrete:

$$E_c = \omega_c^{1.5} 0.43\sqrt{f'_c} \text{ (MPa)} \qquad (4.1)$$

where

$\omega_c = 2446 \text{ kg/m}^3$

f'c = 28 day cylinder compressive strength of concrete

A summary of the input properties for the FE modeling is provided in Table 4.1. The dimensions of the girder were input as keypoints during the development of the model. These keypoints were subsequently joined to form an area, as shown in Fig. 4.3. The created areas were then extruded to the appropriate length and glued to form the volume, as shown in Fig. 4.4. After creating the volume, the model was then meshed to form adequate nodes for loading purposes.

Table 4.1 Material Properties

Concrete Properties	
f'_c (MPa)	44.82
Poisson's Ratio (μ)	0.20
28 day Modulus of Elasticity, E_c (MPa)	33900

4.3.1 Loading

The loading on the bridge was represented by the HL93 specifications for truck and lane loading of the LRFD AASHTO Specifications (AASHTO 1998). The HL93 design loading includes a design lane load of 9.3 kN/m uniformly distributed in the longitudinal direction over a 3.0 m width. The force effects of the design lane load shall not be subject to a dynamic load allowance. The HL93 design loading also includes the following truck loading characteristics: two 145 kN axles spaced between 4.3 and 9.0 m to produce extreme force effects, and one 35 kN axle at 4.3 m from the first 145 kN axle, as shown in Fig. 4.5. The axles were placed at 4.3 m apart to create the maximum moment effect on the girders. A dynamic load allowance was not considered. The design truck loading was placed at locations, which created the maximum moment on the bridge. The placement of the loads for maximum moment was determined using structural analysis and is listed in Table 4.2.

4.4 Straight Bridge Model

To model the eight girders of the bridge, a portion of the slab was glued to the girder model shown in Fig. 4.4. The girder was then copied and glued to simulate an eight-girder bridge with 2.1 m girder spacing. The model was then meshed to specifications for loading purposes.

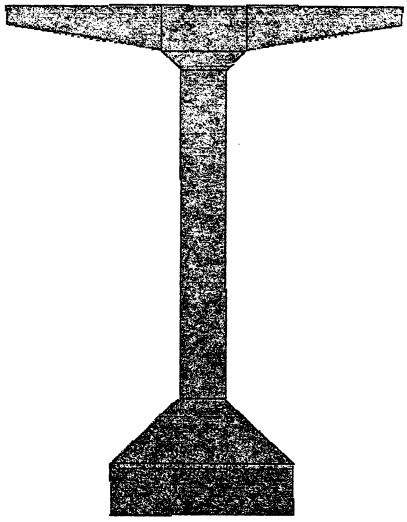

Figure 4.3 Cross-Sectional Area of Florida Bulb Tee 78 Girder

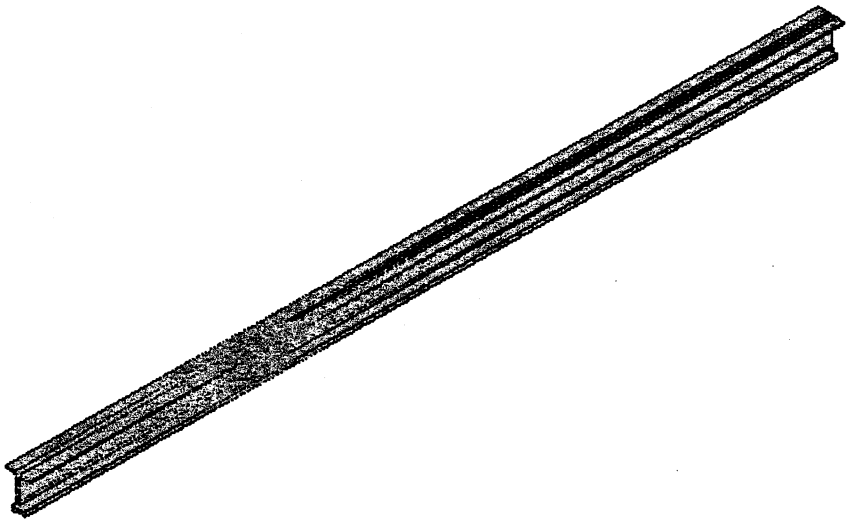

Figure 4.4 Extruded Volume of Girder

4.4.1. End Diaphragm

The dimensions of the diaphragm were obtained from FDOT Structural Research Center. The diaphragm was modeled with 0.2032 m thickness. The diaphragm spans the width of the bridge, and its base is approximately 0.204 m above the base of the girder. The outline of the diaphragm is shown in Fig. 4.6. The diaphragm was created using keypoints that are a reflection of the girder keypoints. These keypoints were then used to create areas and subsequently volumes. These volumes were created at each end of the bridge and were glued together so that the model acts as a single unit.

4.4.2 Spring Placement

To accommodate horizontal movements of the bridge girders, the bearings are designed so that the total thickness of the elastomer in the bearing is equal to or greater than twice the allowable shear deflection. Restraint of movement due to the shear stiffness of the bearing pads results in a moment in the structure. The horizontal restraining effects were calculated taking into account the shear stiffness of the bearings as presented in Eqs. 3.5 and 3.6. The spring stiffness values where calculated for the bearing pad surface. Nine external nodes were created to simulate the compressive element of the bearing pad and three additional external nodes were created for the horizontal stiffness component. Each corner spring element received 1/16 th of the total stiffness. The middle element received 1/8 th of the total stiffness, and the center element received ¼ th of the total stiffness as shown in Fig. 4.7.

The calculated spring stiffness values for the Florida Bulb Tee girder model are shown in Table 4.3.

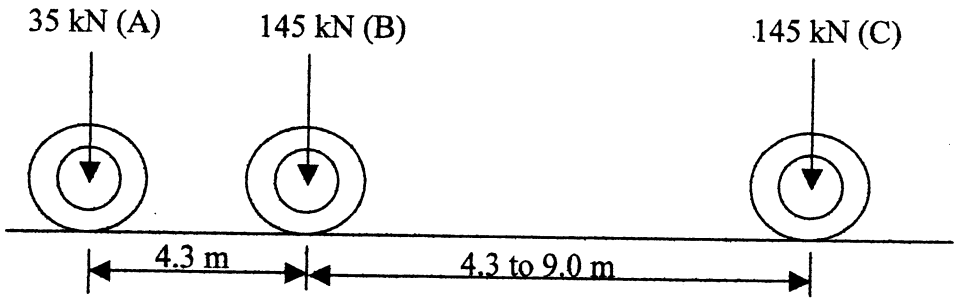

Figure 4.5 HL93 Design Truck Spacing (AASHTO)

Table 4.2 Location of Truck Loads

Girder Length (m)	Girder Spacing (m)	Locations of Design Loads (m)		
		A	B	C
45	2.1	17.47	21.77	26.07

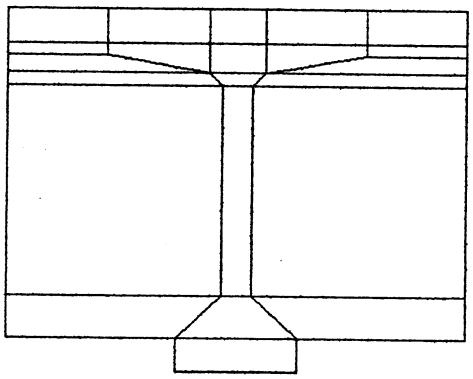

Figure 4.6 Outline of Diaphragm

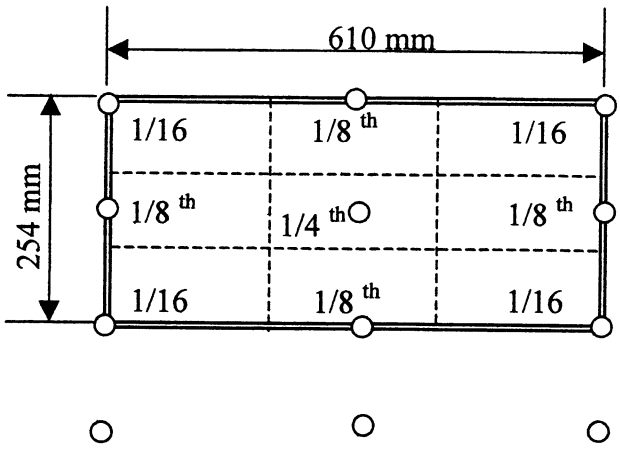

Figure 4.7 Tributary Area for Placement of Spring Elements

Table 4.3 Spring Stiffness Values of Florida Bulb Tee Girder Model

Boundary Conditions	Number of Elements	Fraction of Total Stiffness	Spring Stiffness Values (N/mm^2)				
			Roller	0.655	1.379	3.448	6.895
Compressive Spring Stiffness, K_c (N/mm)							
Vertical Elements	72	Full	-	1.50E6	3.15E6	7.88E6	1.58E7
Corner Springs	32	1/16	∞	93529	196904	492261	984521
Middle Springs	32	1/8	∞	187059	187059	393808	1969042
Center Springs	8	¼	∞	374118	787617	1969042	3938084
Horizontal Spring Stiffness, K_h (N/mm)							
Horizontal Elements	72	Full	-	2706	2706	5697	28487
Corner Springs	32	1/16	0	169	169	356	1780
Middle Springs	32	1/8	0	338	338	712	3560
Center Springs	8	¼	0	677	677	1424	7122

4.5 Skewed Bridge

The cross sectional area of the original girder was used to create the outline of the skewed girder. This girder was then extruded on the complementary angle of the intended skew. The extrusion parameters were calculated on the premise of maintaining the 45 m length of the bridge. An additional effort was made to model the bearing pads precisely due to their placement on a skewed bridge. The presence of intermediate diaphragms is linked to the skewness of the bridge, according to AASHTO specifications. When the skew angle is greater than 30°, intermediate diaphragms per AASHTO specifications are to be provided. Intermediate diaphragms are not needed when the angle is less than 30°. The models were tested with skew angles of 15°, 30°, 45°, and 60°. The end and intermediate diaphragms were placed accordingly. The location of the skewed spring element nodes is shown in Fig. 4.8.

4.5.1 Intermediate Diaphragms

The intermediate diaphragms were modeled similar to the end diaphragms as shown in Fig. 4.9. The diaphragms were placed perpendicular to the girder between the webs of each girder. They were placed at 1/3 points along the girder length.

4.6 Temperature

The temperature was input as a load on the elements using the ANSYS BFE command. The BFE command applies a body load to an element. This body load can be applied as a temperature for structural applications. The command works in conjunction with the thermal coefficient, which is input as a material property.

The temperature data was obtained from the FDOT Structures Design Guidelines. (FDOT 1999) The guidelines specify a low temperature of 280.15°K (7°C) and a high temperature of

temperature for structural applications. The command works in conjunction with the thermal coefficient, which is input as a material property.

The temperature data was obtained from the FDOT Structures Design Guidelines. (FDOT 1999) The guidelines specify a low temperature of 280.15°K (7°C) and a high temperature of 308.15°K (35°C) with a thermal coefficient of 0.0000090 / °K. The temperature difference was input as a body load onto the concrete elements.

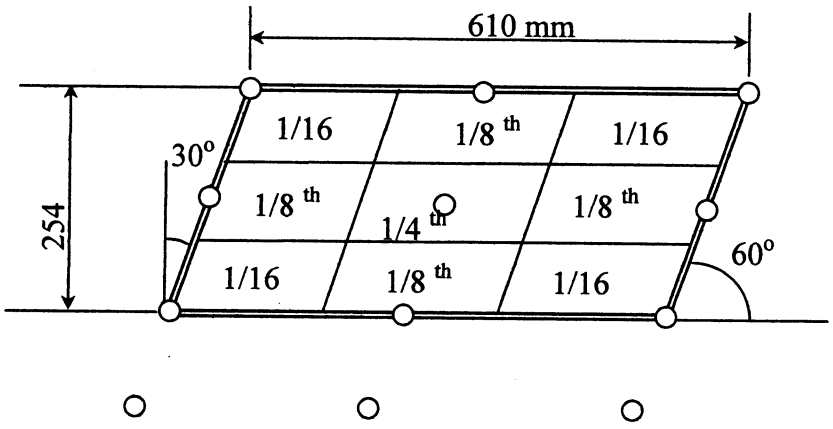

Figure 4.8 Tributary Area and Placement for Skewed Spring Elements

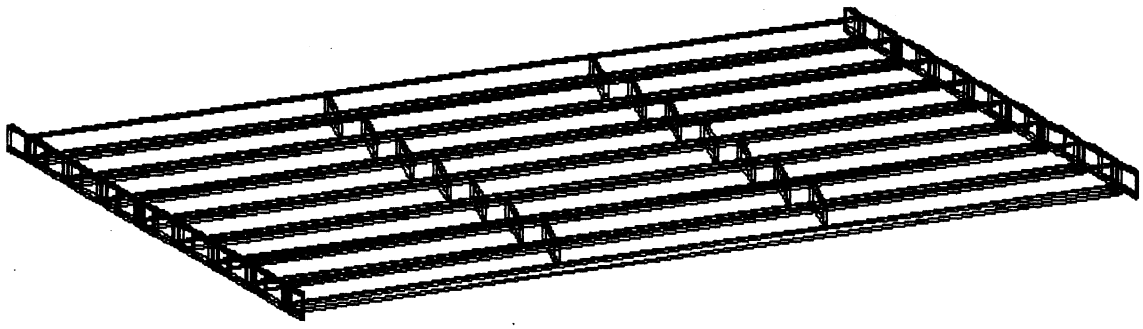

Figure 4.9 Typical View of the Intermediate Diaphragms

CHAPTER 5

RESULTS AND DISCUSSION

5.1 Parametric Matrix

A parametric study was adopted herein to determine the various parameters affecting the performance of the model bridge. Towards this end, several parametric matrices were developed and used in this study. These parameters include the bearing stiffness of the spring elements, skewness, the presence of intermediate diaphragms, and the temperature changes. The parametric analysis was performed through the comparison of deflections, stresses, and vertical and horizontal reactions of the spring elements. The parametric matrices are presented in Tables 5.1 - 5.4.

Table 5.1 Effect of Skewness and Bearing Stiffness (Template)

Length = 45 m, Spacing = 2.1 m with End Diaphragm only

Skew Angle (Degrees)	Shear Modulus (G), GPa				
	Simply Supported	0.655	1.379	3.447	6.895
0					
15					
30					
45					
60					

Table 5.2 Effect of Intermediate Diaphragms (Template)

Length = 45 m, Spacing = 2.1 m with End and Intermediate Diaphragms

Skew Angle (Degrees)	Shear Modulus (G), GPa				
	Simply Supported	0.655	1.379	3.447	6.895
0					
15					
30					
45					
60					

Table 5.3 Effect of Temperature Change (Negative Differential - Template)

Length = 45 m, Spacing = 2.1 m with End Diaphragm only

Skew Angle (Degrees)	Shear Modulus (G), GPa				
	Simply Supported	0.655	1.379	3.447	6.895
0					
15					
30					
45					
60					

Table 5.4 Effect of Temperature Change (Positive Differential - Template)

Length = 45 m, Spacing = 2.1 m with End Diaphragm only

Skew Angle (Degrees)	Shear Modulus (G), GPa				
	Simply Supported	0.655	1.379	3.447	6.895
0					
15					
30					
45					
60					

5.2 Effect of Skewness and Bearing Stiffness

The combined effect of skewness and bearing stiffness results are presented in Tables 5.5 – 5.12. A comparison of these results are graphically presented in Figs. 5.1 – 5.4.

Table 5.5 Combined Effect of Skewness and Bearing Stiffness (Maximum Deflection, mm)

Length = 45 m, Spacing = 2.1 m with End Diaphragm only

Skew Angle (Degrees)	Shear Modulus (G), GPa				
	Simply Supported	0.655	1.379	3.447	6.895
0	14.90	16.30	16.08	15.66	15.11
15	15.18	16.51	16.28	15.83	15.28
30	16.11	17.09	16.78	16.18	15.47
45	18.00	18.35	18.00	17.28	16.43
60	22.39	21.44	20.76	19.28	17.58

Table 5.6 Percent Difference in Maximum Deflection Due to Skewness and Bearing Stiffness (All Values Compared to Non-Skewed Bridge)

Length = 45 m, Spacing = 2.1 m with End Diaphragm only

Skew Angle (Degrees)	Shear Modulus (G), GPa				
	Simply Supported	0.655	1.379	3.447	6.895
15	1.88	1.29	1.24	1.09	1.13
30	8.12	4.85	4.35	3.32	2.38
45	20.81	12.58	11.94	10.34	8.74
60	50.26	31.53	29.10	23.12	16.35

Table 5.7 Combined Effect of Skewness and Bearing Stiffness (Maximum Tensile Stresses, MPa)

Length = 45 m, Spacing = 2.1 m with End Diaphragm only

Skew Angle (Degrees)	Shear Modulus (G), GPa				
	Simply Supported	0.655	1.379	3.447	6.895
0	4.20	4.55	4.52	4.43	4.32
15	5.17	5.60	5.55	5.45	5.31
30	6.01	6.34	6.28	6.12	5.93
45	6.81	6.91	6.84	6.66	6.44
60	7.60	7.41	7.28	6.96	6.57

Table 5.8 Percent Difference in Maximum Tensile Stresses Due to Skewness and Bearing Stiffness (All Values Compared to Straight Bridge)

Length = 45 m, Spacing = 2.1 m with End Diaphragm only

Skew Angle (Degrees)	Shear Modulus (G), GPa				
	Simply Supported	0.655	1.379	3.447	6.895
15	23.10	23.08	22.79	23.02	22.92
30	43.10	39.34	38.94	38.15	37.27
45	62.14	51.87	51.33	50.34	49.07
60	80.95	62.86	61.06	57.11	52.08

Table 5.9 Combined Effect of Skewness and Bearing Stiffness (Total Vertical Reaction, kN)

Length = 45 m, Spacing = 2.1 m with End Diaphragm only

Skew Angle (Degrees)	Shear Modulus (G), GPa				
	Simply Supported	0.655	1.379	3.447	6.895
0	1487	1487	1487	1487	1487
15	1482	1483	1483	1483	1483
30	1484	1484	1484	1484	1484
45	1485	1485	1485	1485	1485
60	1487	1487	1487	1487	1487

Table 5.10 Vertical Reactions Across Bridge (kN) for G = 0.655 GPa

Length = 45 m, Spacing = 2.1 m with End Diaphragm only

Skew Angle (Degrees)		Girders							
		1	2	3	4	5	6	7	8
15	Left Support	-6.89	54.04	123.01	174.91	190.56	164.46	87.37	-35.18
	Right Support	-32.48	84.82	158.75	183.93	169.12	119.64	53.33	-6.63
30	Left Support	145.47	100.88	78.03	128.45	103.64	65.47	66.00	62.33
	Right Support	-37.69	116.69	162.03	176.90	154.11	109.62	35.94	15.75
45	Left Support	38.77	42.01	74.48	125.98	160.61	173.92	131.53	-13.22
	Right Support	-14.01	131.68	176.91	164.17	126.76	76.86	47.98	36.10
60	Left Support	58.28	50.40	64.01	94.15	124.44	147.53	136.08	70.85
	Right Support	72.00	134.49	146.11	123.55	93.44	63.49	49.97	58.19

Table 5.11 Combined Effect of Skewness and Bearing Stiffness (Total Horizontal Reactions, Left Support, kN)

Length = 45 m, Spacing = 2.1 m with End Diaphragm only

Skew Angle (Degrees)	Shear Modulus (G), GPa				
	Simply Supported	0.655	1.379	3.447	6.895
0	9.00	23.76	49.01	116.41	225.59
15	10.00	22.98	47.39	112.54	210.01
30	6.00	21.38	43.95	103.20	190.04
45	6.40	19.19	39.45	92.94	171.66
60	1.69	16.03	32.62	75.08	134.78

Table 5.12 Combined Effect of Skewness and Bearing Stiffness (Total Horizontal Reactions, Right Support, kN)

Length = 45 m, Spacing = 2.1 m with End Diaphragm only

Skew Angle (Degrees)	Shear Modulus (G), GPa				
	Simply Supported	0.655	1.379	3.447	6.895
0	0	23.76	49.01	116.41	225.59
15	0	22.98	47.39	112.54	210.01
30	0	21.58	44.15	103.40	190.25
45	0	19.44	39.90	93.81	172.97
60	0	16.03	32.62	75.08	134.78

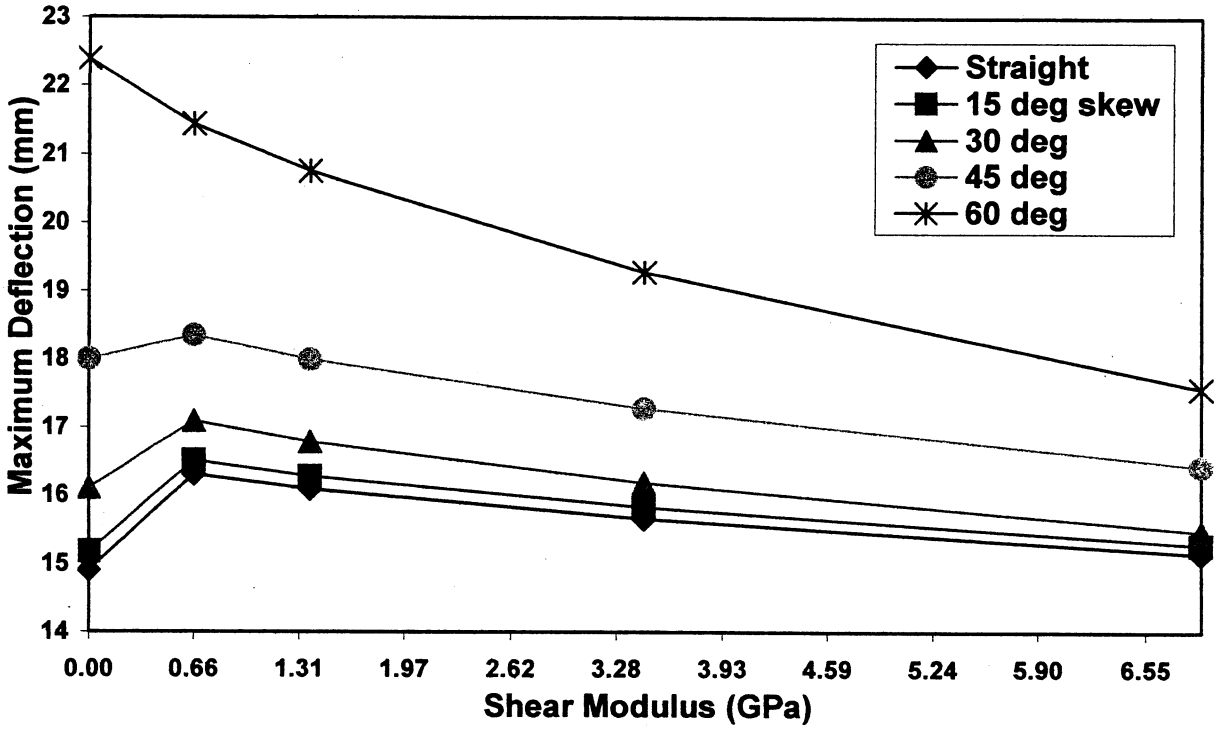

Figure 5.1 Maximum Midpoint Deflections for Various Bearing Stiffness and Skew Angles (End Diaphragms Only)

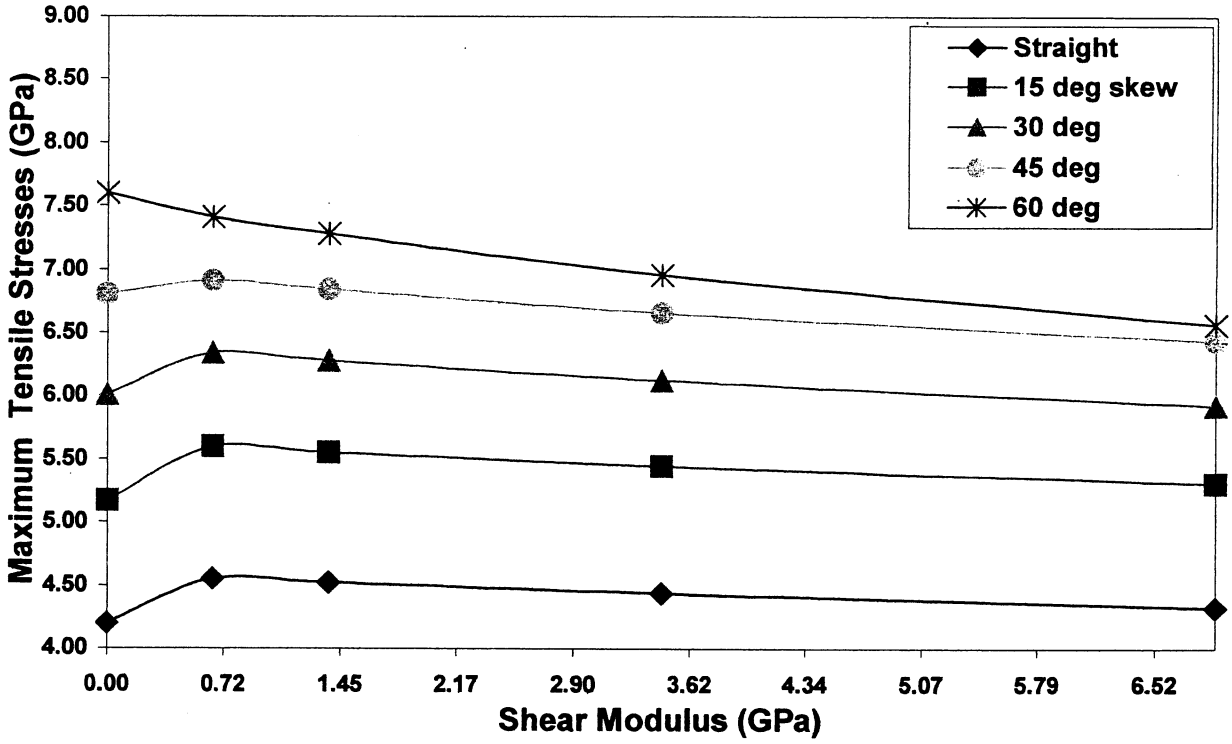

Figure 5.2 Maximum Tensile Stresses for Various Bearing Stiffness and Skew Angles (End Diaphragms Only)

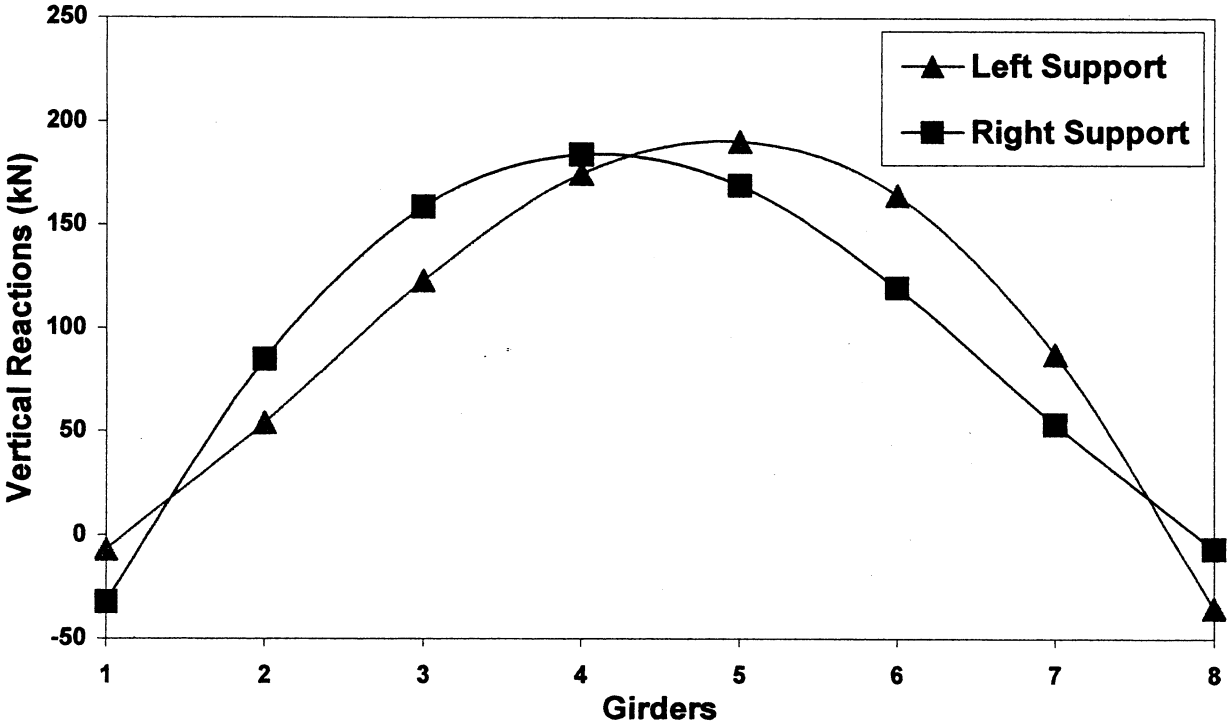

Figure 5.3 Comparison of Vertical Reactions Across Bridge Girders for 15° Skew and G = 0.655 GPa (End Diaphragms Only)

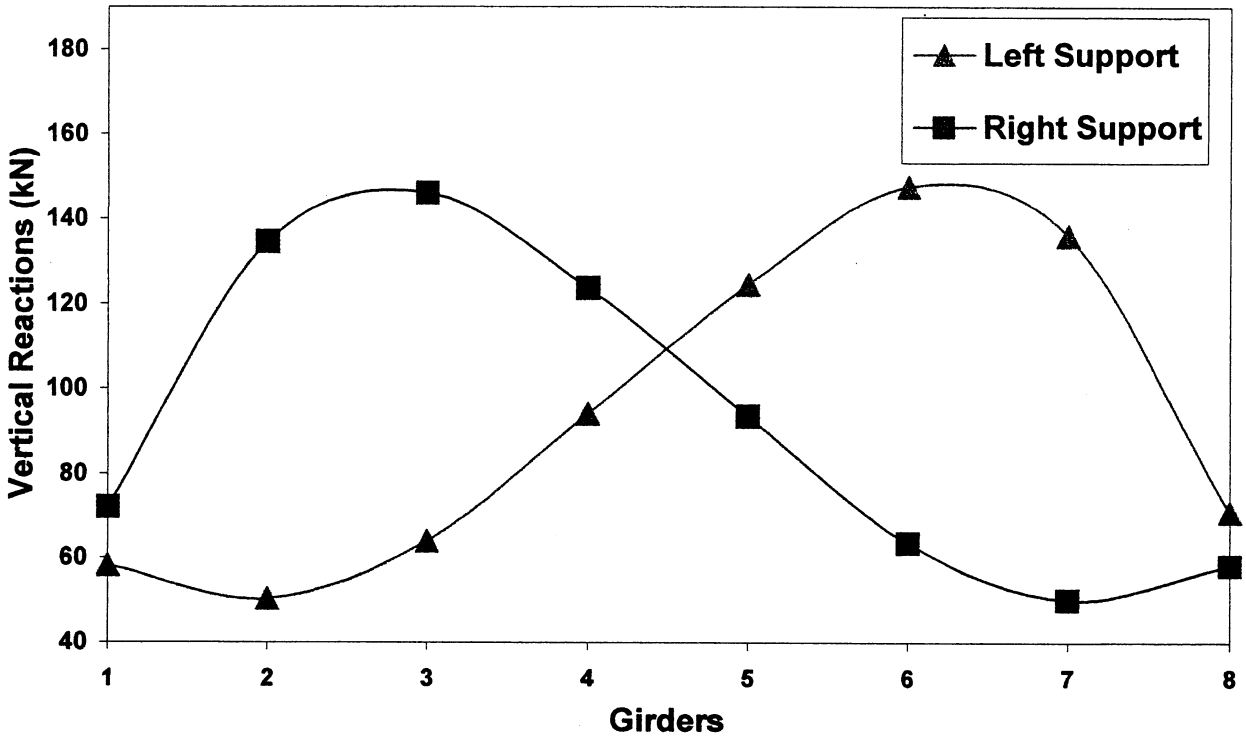

Figure 5.4 Comparison of Vertical Reactions Across Bridge Girders for 60° Skew and G = 0.655 GPa (End Diaphragms Only)

5.2.1 Discussion

The results illustrated in Table 5.5 and Fig. 5.1 indicates a general increase in maximum deflection as the skew angle increases. The deflections are found to decrease with increasing bearing stiffness. As compared to the new bearing stiffness, (0.655 Gpa), a ten fold stiffness increase to 6.895 GPa results in deflection decrease of about 7 to 18 % for skew angles of 0° and 60°, respectively. The maximum deflections are found to increase by 50% if the skew angle is increased to 60° for the simple support conditions. This increase is less pronounced (about 16%) for a shear modulus of 6.895 GPa. The simply supported condition is considered more rigid than the spring elements; this support condition does not allow any vertical end deflection. The deflection results for the bearing pad spring models include the effect of vertical end deflection due to spring compression. This causes the deflection of the simply supported

condition to appear less than that for the spring bearings. This effect becomes less pronounced as the skew angle increases. This effect may be corrected by subtracting the vertical spring deformations from the deflection results. During the research, AASHTO distribution reduction factor values for skew girders (AASHTO 4.6.2) were analyzed and found to have minimal effect on the results (AASHTO 1998). The factors ranged from 0.99 for a 30° skew to 0.98 for a 60° skew bridge. Recent research on nonlinear analysis of reinforced concrete skew slabs found results that show the same pattern of increasing deflection and tensile stresses as the skew angle increased (Nizamud-doulah 2000).

The results shown in Table 5.7 and Fig. 5.2 indicate a decrease in the maximum tensile stresses as the bearing stiffness increases and an increase as the skew angle increases. The simply supported condition follows the same pattern as shown in the deflection results. Table 5.8 indicates that as the skew angle increases, the midpoint tensile stresses show an increase of over 80% for the 60 degree skew when compared with the straight bridge. These results indicate that the maximum tensile stresses increase at a greater rate than the deflection.

Table 5.9 shows the total vertical reactions exerted on the bridge girders. As expected, the vertical reactions remain almost constant indicating that the spring supports are carrying the full truck and lane loading applied to the beam. Table 5.10 and Figs. 5.3 and 5.4 compare the vertical reactions on opposing ends of the girder. These figures indicated that uplift is occurring due to the skew angle. This uplift is occurring only at the side supports and results in total separation for the lower skew angles on one or both girder ends. As the skew angle increases, the uplift gradually reduces and disappears at the 60° skew angle as shown in Table 5.10.

Tables 5.11 and 5.12 present the horizontal reactions for various bearing stiffnesses and skew angles. These reactions are equal but opposite indicating that the bridge system is not

moving laterally. It is observed that the horizontal reactions increase in almost direct ratio to the increase in bearing stiffness. There is also a decrease in horizontal reactions with skew angle increase.

5.3 Effect of Intermediate Diaphragms

The effects of the intermediate diaphragm on the skewness and bearing stiffness results are presented in Tables 5.13 – 5.20. Comparisons of these results are graphically presented in Figs. 5.5 – 5.10. The results compare the deflection, stresses and vertical and horizontal reactions. The results show the comparison of the intermediate plus end diaphragm results to the end diaphragm only results previously presented.

Table 5.13 Effect of Intermediate Diaphragms (Maximum Deflection ,mm)

Length = 45 m, Spacing = 2.1 m with End and Intermediate Diaphragms

Skew Angle (Degrees)	Shear Modulus (G), GPa				
	Simply Supported	0.655	1.379	3.447	6.895
0	13.34	13.52	13.35	12.99	12.56
15	14.11	14.58	14.38	13.98	13.50
30	15.05	15.23	14.96	14.40	13.76
45	17.13	17.16	16.83	16.15	15.38
60	21.29	20.26	19.59	18.15	16.48

Table 5.14 Percent Difference in Maximum Deflection Due to Skewness and Bearing Stiffness (All Values Compared to Straight Bridge)

Length = 45 m, Spacing = 2.1 m with End and Intermediate Diaphragms

Skew Angle (Degrees)	Shear Modulus (G), GPa				
	Simply Supported	0.655	1.379	3.447	6.895
15	5.77	7.84	7.72	7.62	7.48
30	12.82	12.65	12.06	10.85	9.55
45	28.41	26.92	26.07	24.33	22.45
60	59.60	49.85	46.74	39.72	31.21

Table 5.15 Effect of Intermediate Diaphragms (Maximum Tensile Stresses, MPa)

Length = 45 m, Spacing = 2.1 m with End and Intermediate Diaphragms

Skew Angle (Degrees)	Shear Modulus (G), GPa				
	Simply Supported	0.655	1.379	3.447	6.895
0	3.75	3.80	3.78	3.71	3.62
15	4.66	4.77	4.74	4.65	4.53
30	5.50	5.56	5.51	5.36	5.19
45	6.58	6.58	6.51	6.34	6.12
60	7.70	7.52	7.38	7.06	6.67

Table 5.16 Percent Difference in Maximum Tensile Stresses Due to Skewness and Bearing Stiffness (All Values Compared to Straight Bridge)

Length = 45 m, Spacing = 2.1 m with End and Intermediate Diaphragms

Skew Angle (Degrees)	Shear Modulus (G), GPa				
	Simply Supported	0.655	1.379	3.447	6.895
15	24.27	25.53	25.40	25.34	25.14
30	46.67	46.32	45.77	44.47	43.37
45	75.47	73.16	72.22	70.89	69.06
60	105.33	97.89	95.24	90.30	84.25

Table 5.17 Effect of Intermediate Diaphragms (Total Vertical Reaction, kN)

Length = 45 m, Spacing = 2.1 m with End and Intermediate Diaphragms

Skew Angle (Degrees)	Shear Modulus (G), GPa				
	Simply Supported	0.655	1.379	3.447	6.895
0	1487	1487	1487	1487	1487
15	1483	1483	1483	1483	1483
30	1484	1484	1484	1484	1484
45	1485	1485	1485	1485	1485
60	1487	1487	1487	1487	1487

Table 5.18 Vertical Reactions Across Bridge (kN)

Length = 45 m, Spacing = 2.1 m with End and Intermediate Diaphragms

Skew Angle (Degrees)		Girders							
		1	2	3	4	5	6	7	8
15	Left Support	22.38	61.09	108.94	146.31	161.93	150.13	95.89	5.58
	Right Support	7.34	95.04	145.20	154.65	139.65	104.55	60.10	23.93
30	Left Support	33.75	56.52	96.36	136.76	157.95	147.61	108.86	12.38
	Right Support	100.66	54.44	88.88	119.37	74.14	90.35	105.58	99.99
45	Left Support	45.97	51.13	80.32	116.90	142.68	153.41	123.03	24.76
	Right Support	26.38	125.17	154.81	142.35	115.16	82.05	51.36	49.05
60	Left Support	56.88	53.48	66.57	92.75	118.02	137.52	129.52	91.24
	Right Support	91.91	129.32	136.24	116.13	90.99	65.82	54.01	57.01

Table 5.19 Effect of Intermediate Diaphragms (Total Horizontal Reaction, Left Support, kN)

Length = 45 m, Spacing = 2.1 m with End and Intermediate Diaphragms

Skew Angle (Degrees)	Shear Modulus (G), GPa				
	Simply Supported	0.655	1.379	3.447	6.895
0	1.00	23.49	48.46	115.20	215.35
15	6.00	22.89	47.21	112.12	209.24
30	3.60	21.31	43.82	102.91	189.54
45	0.78	19.18	39.44	92.97	171.57
60	0.90	15.92	32.39	74.56	133.87

Table 5.20 Effect of Intermediate Diaphragms (Total Horizontal Reaction, Right Support, kN)

Length = 45 m, Spacing = 2.1 m with End Diaphragm and Intermediate Diaphragms

Skew Angle (Degrees)	Shear Modulus (G), GPa				
	Simply Supported	0.655	1.379	3.447	6.895
0	0	23.48	48.46	115.20	215.35
15	0	22.89	47.21	112.12	209.24
30	0	21.52	44.02	103.11	189.75
45	0	19.42	39.86	93.80	172.85
60	0	15.92	32.39	74.56	134.87

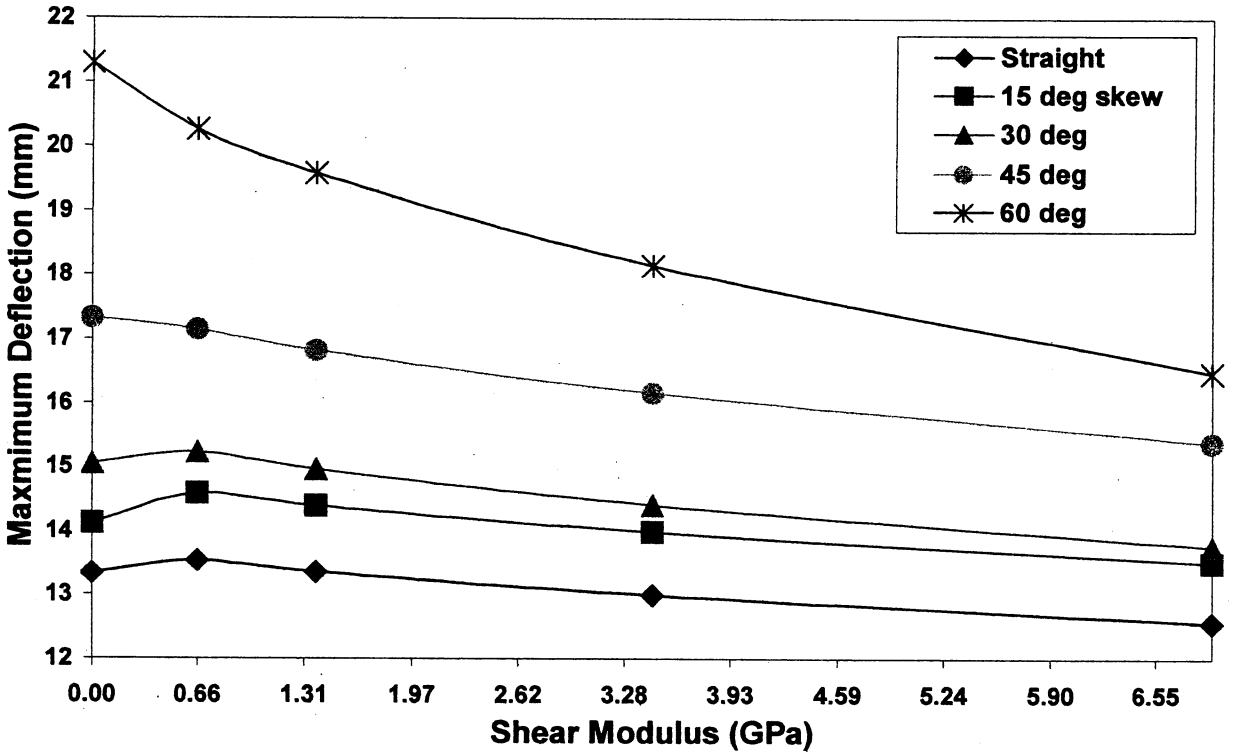

Figure 5.5 Maximum Deflections for Various Bearing Stiffness and Skew Angles (End and Intermediate Diaphragms)

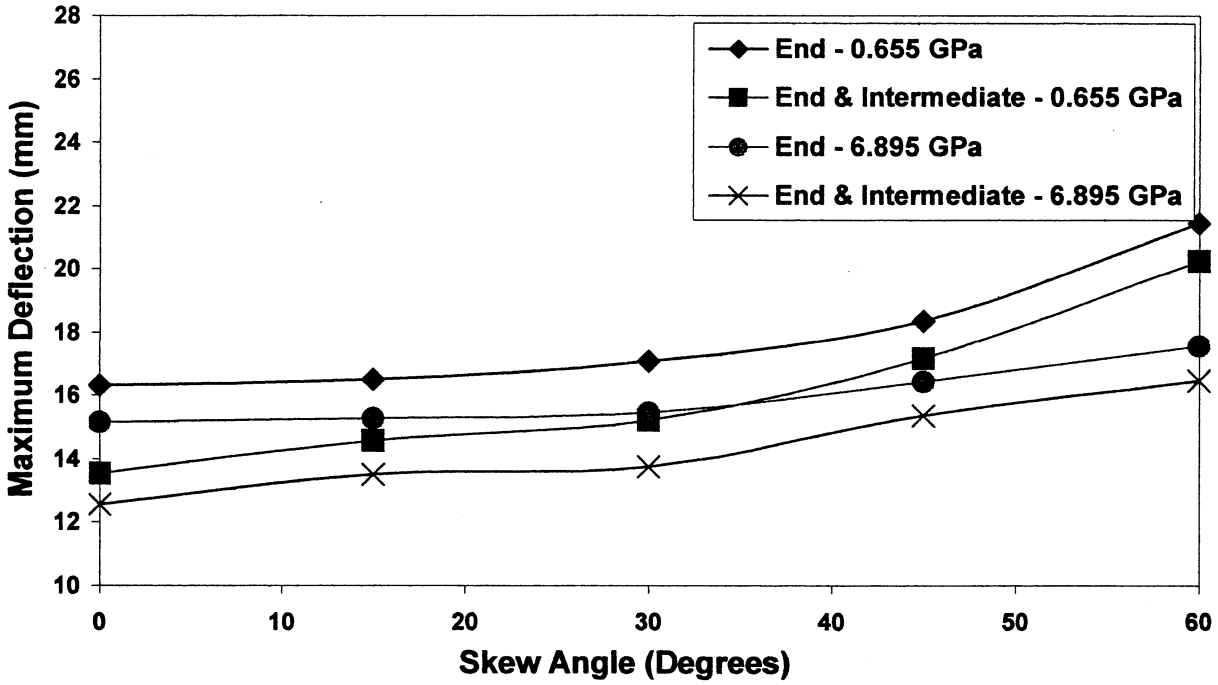

Figure 5.6 Comparison of Maximum Deflection for Various Skew Angles with Intermediate and End Diaphragms for G = 0.655 and 6.895 GPa

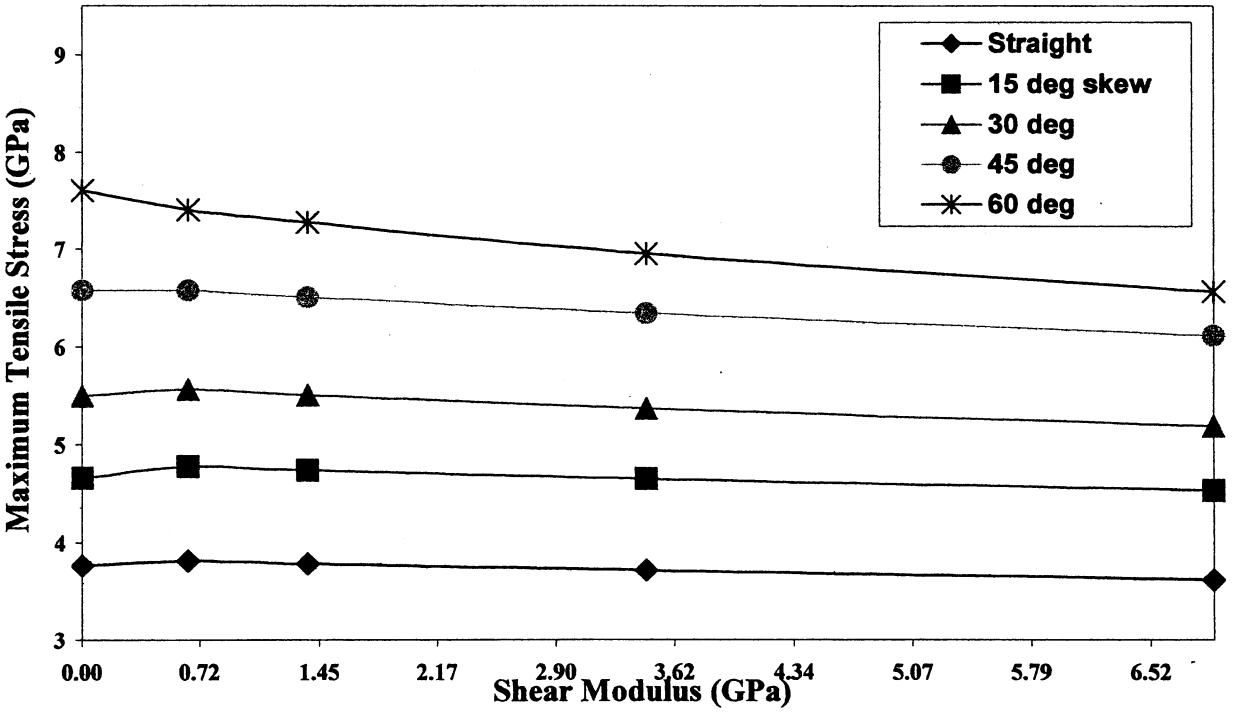

Figure 5.7 Maximum Tensile Stresses for Various Bearing Stiffness and Skew Angles (Intermediate Diaphragms)

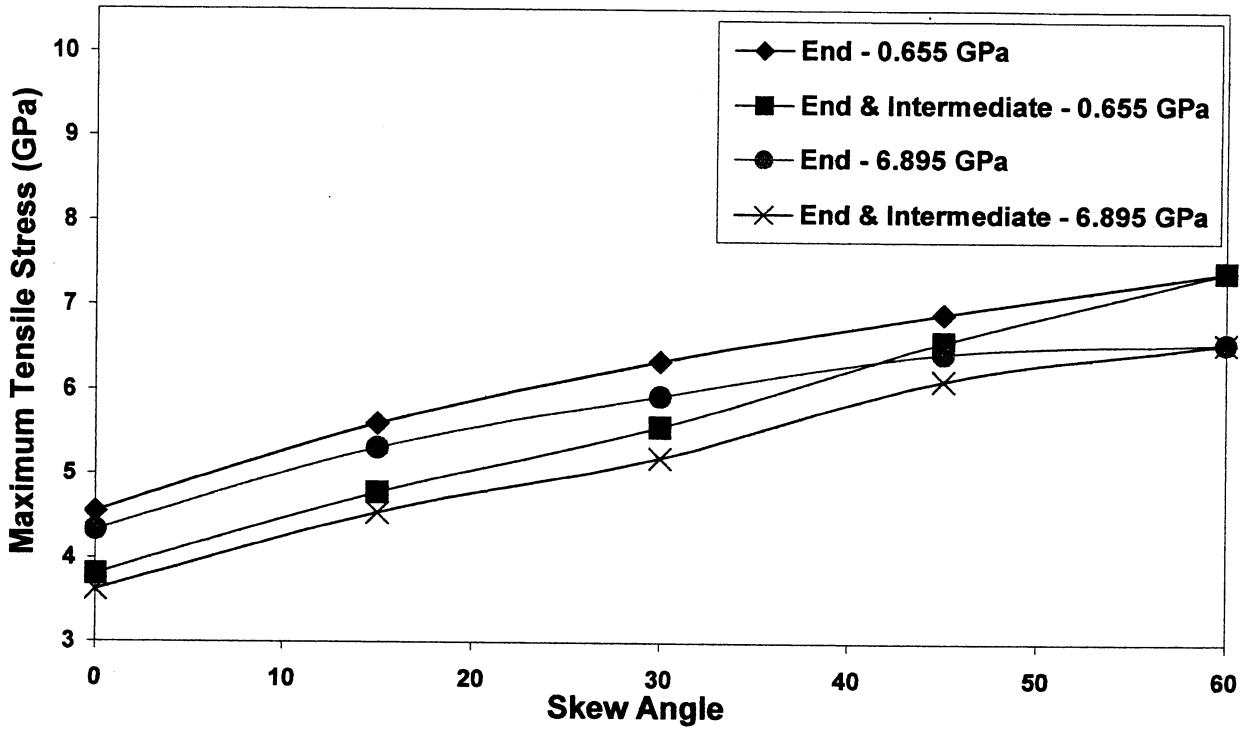

Figure 5.8 Comparison of Maximum Tensile Stresses for Various Skew Angles with Intermediate Diaphragms for G = 0.655 and 6.895 GPa

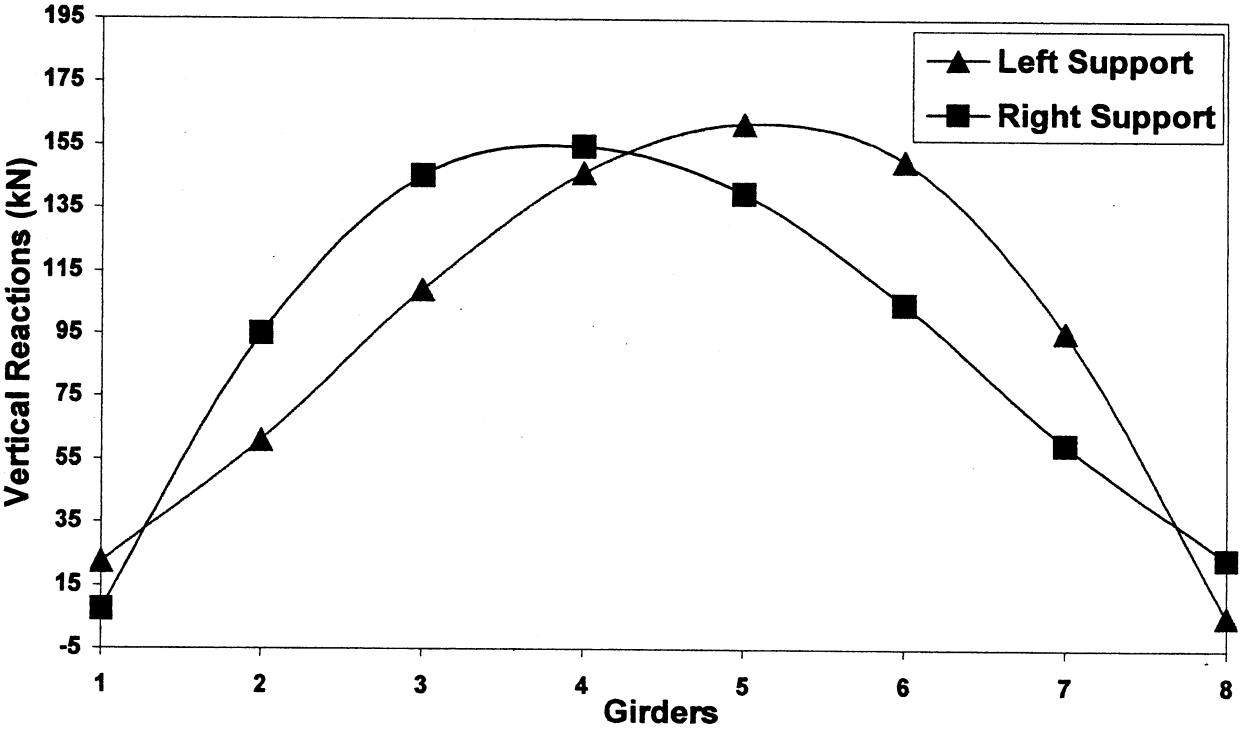

Figure 5.9 Comparison of Vertical Reactions Across Bridge Girder for 15° Skew (End and Intermediate Diaphragms)

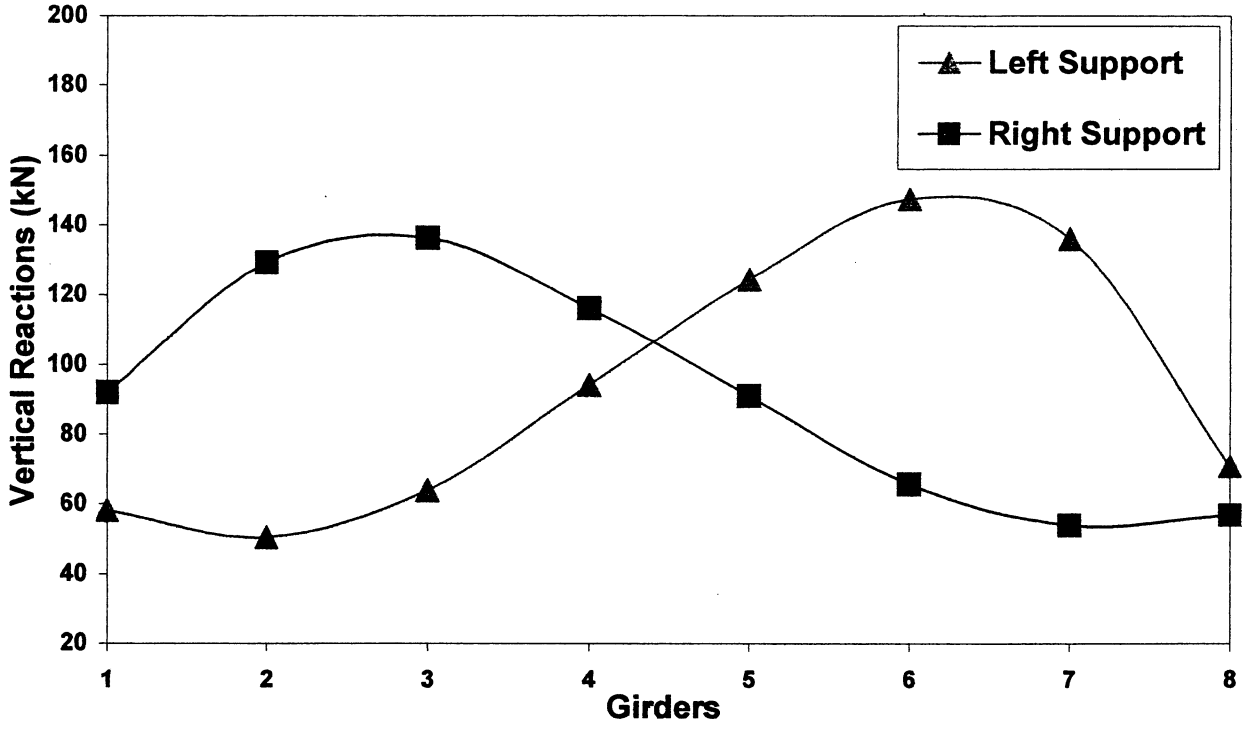

Figure 5.10 Comparison of Vertical Reactions Across Bridge Girder for 60° Skew (End and Intermediate Diaphragms)

5.3.1 Discussion

The results illustrated in Table 5.13 and Fig. 5.5 indicates an increase in maximum deflection as the skew angles increase. As the bearing stiffnesses increases, a decrease in maximum deflection occurs. This trend is similar to the one for end diaphragms only. The maximum deflections increase by 31 to 60% for the 60° skew when compared with the straight bridge. As compared to the new bearing stiffness, (0.655 Gpa), a ten fold stiffness increase to 6.895 GPa results in deflection decrease of about 7 to 18 % for skew angles of 0° and 60°, respectively. A comparison of Tables 5.5 and 5.13 show an overall decrease in deflection due to the inclusion of an intermediate diaphragm on all models. As stated previously, these deflection results for the bearing pad spring models include the effect of vertical end deformation due to spring compression. The simply supported condition does not allow for vertical movements.

Figure 5.6 shows that as the skew angle increases, the effect of the intermediate diaphragm decrease in reducing deflections. Intermediate diaphragms reduce maximum deflections by about 17% for straight bridges, whereas the reduction was between 4 - 6% for 60° skew.

Table 5.15 and Fig. 5.7 indicate a decrease in maximum tensile stresses as the bearing stiffness increases and an increase as the skew angle increases. A comparison of Tables 5.6 and 5.15 indicate a decrease in tensile stresses with the application of the intermediate diaphragms for all cases except for a 60° skew angle. Figure 5.8 shows the effect of the intermediate diaphragms as the skew angle increases for bearing stiffness' of G = 0.655 GPa and G = 6.895 GPa. This figure indicates that as the skew angle increases the difference between the maximum tensile stresses decreases.

Table 5.17 shows the total vertical reaction of each bridge system and shows that the springs are supporting the entire load. The horizontal reaction details are presented in Tables 5.19 and 5.20. Table 5.18, and Figs. 5.9 and 5.10 show that the uplift effect is eliminated due to the skew angles utilizing the end and intermediate diaphragms.

5.4 Effect of Temperature Changes

The effects of temperature changes on various parameters are presented in Tables 5.21 – 5.33. Comparisons of these results are presented graphically in Figs. 5.11 – 5.18. The results presented compare the deflection, stresses and vertical and horizontal reactions for both a positive and negative temperature differential. A negative and positive temperature differential of $\pm$ 28 °C was applied to the models as body loads. The truck loads were retained for the thermal modeling.

Table 5.21 Effect of Temperature Change (Positive Temperature Differential, Maximum Deflection, mm)

Length = 45 m, Spacing = 2.1 m with End Diaphragm only

Skew Angle	Bearing Stiffness				
	Simply Supported	G = 0.655 GPa	G = 1.379 GPa	G = 3.447 GPa	G = 6.895 GPa
0	15.09	15.81	15.35	14.30	12.84
15	15.39	16.00	15.52	14.40	12.85
30	16.22	16.48	15.87	14.47	12.59
45	18.12	17.78	16.98	15.09	12.52
60	22.22	20.46	18.96	15.40	10.77

Table 5.22 Effect of Temperature Change (Negative Temperature Differential, Maximum Deflection, mm)

Length = 45 m, Spacing = 2.1 m with End Diaphragm only

Skew Angle	Bearing Stiffness				
	Simply Supported	G = 0.655 GPa	G = 1.379 GPa	G = 3.447 GPa	G = 6.895 GPa
0	10.57	9.78	9.87	10.19	10.76
15	14.96	17.01	17.03	17.25	17.71
30	15.99	17.70	17.69	17.88	18.35
45	17.89	18.92	19.01	19.47	20.35
60	21.95	21.80	21.93	22.54	23.77

Table 5.23 Effect of Temperature Change (Positive Temperature Differential, Maximum Tensile Stresses, GPa)

Length = 45 m, Spacing = 2.1 m with End Diaphragm only

Skew Angle	Bearing Stiffness				
	Simply Supported	G = 0.655 GPa	G = 1.379 GPa	G = 3.447 GPa	G = 6.895 GPa
0	4.19	4.49	4.40	4.15	3.79
15	5.16	5.52	5.40	5.09	4.65
30	5.94	6.24	6.09	5.69	5.13
45	6.69	6.84	6.65	6.17	5.47
60	7.63	7.53	7.25	6.55	5.59

Table 5.24 Effect of Temperature Change (Negative Temperature Differential, Maximum Tensile Stresses, GPa)

Length = 45 m, Spacing = 2.1 m with End Diaphragm only

Skew Angle	Bearing Stiffness				
	Simply Supported	G = 0.655 GPa	G = 1.379 GPa	G = 3.447 GPa	G = 6.895 GPa
0	4.20	4.61	4.63	4.71	4.85
15	5.19	5.66	5.70	5.79	5.97
30	6.09	6.42	6.45	6.56	6.75
45	7.02	7.07	7.13	7.31	7.60
60	8.07	7.86	7.93	8.12	8.46

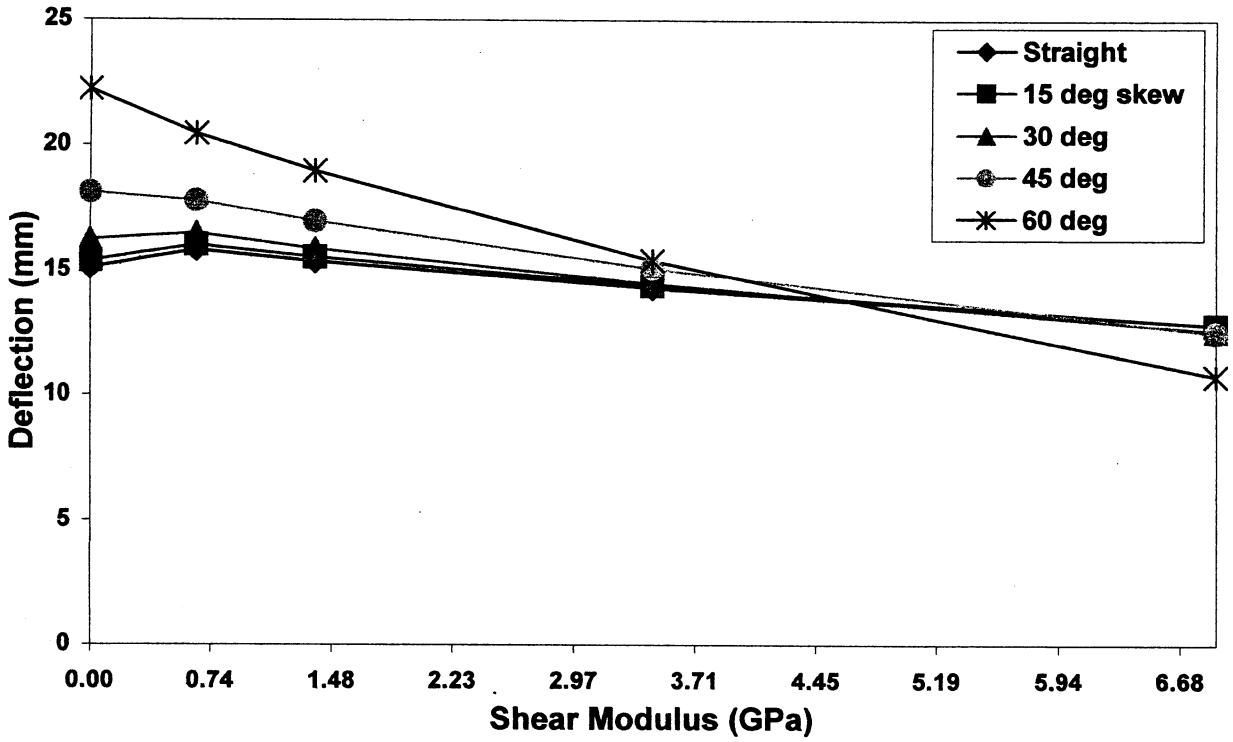

Figure 5.11 Maximum Midpoint Deflections for Various Bearing Stiffness and Skew Angles, Positive Temperature Differential (End Diaphragms Only)

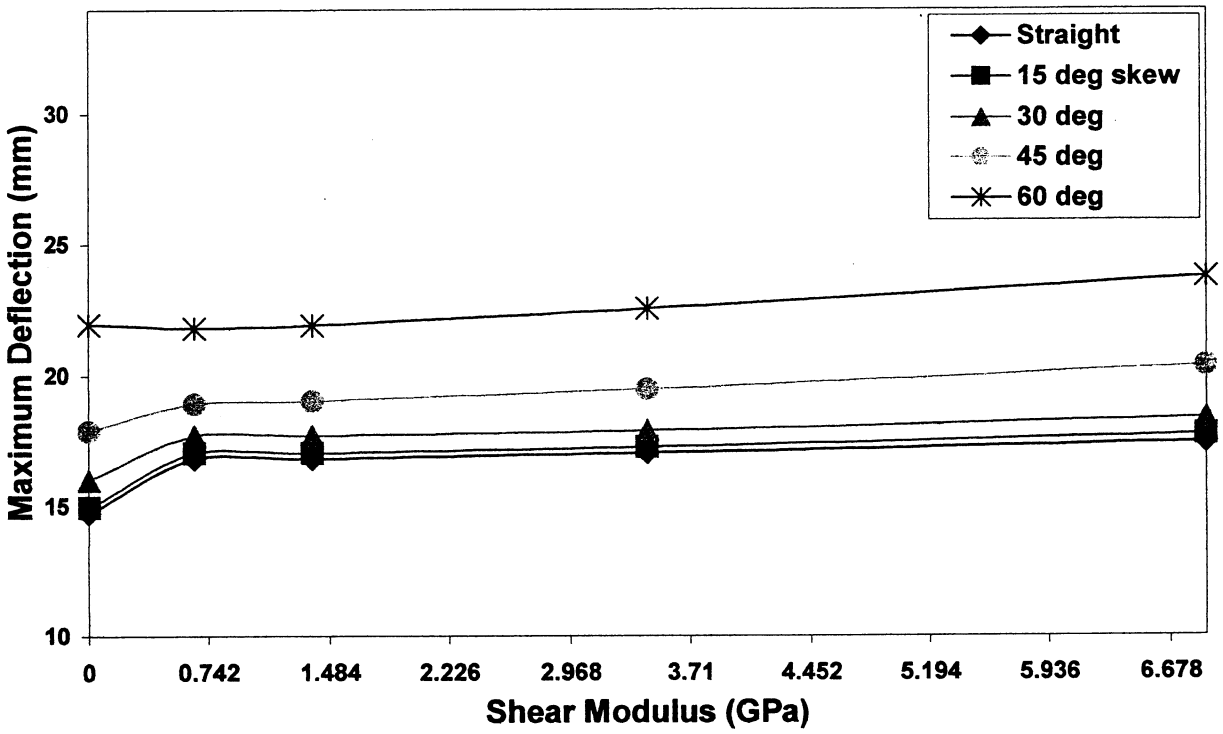

Figure 5.12 Maximum Midpoint Deflections for Various Bearing Stiffness and Skew Angles, Negative Temperature Differential (End Diaphragms Only)

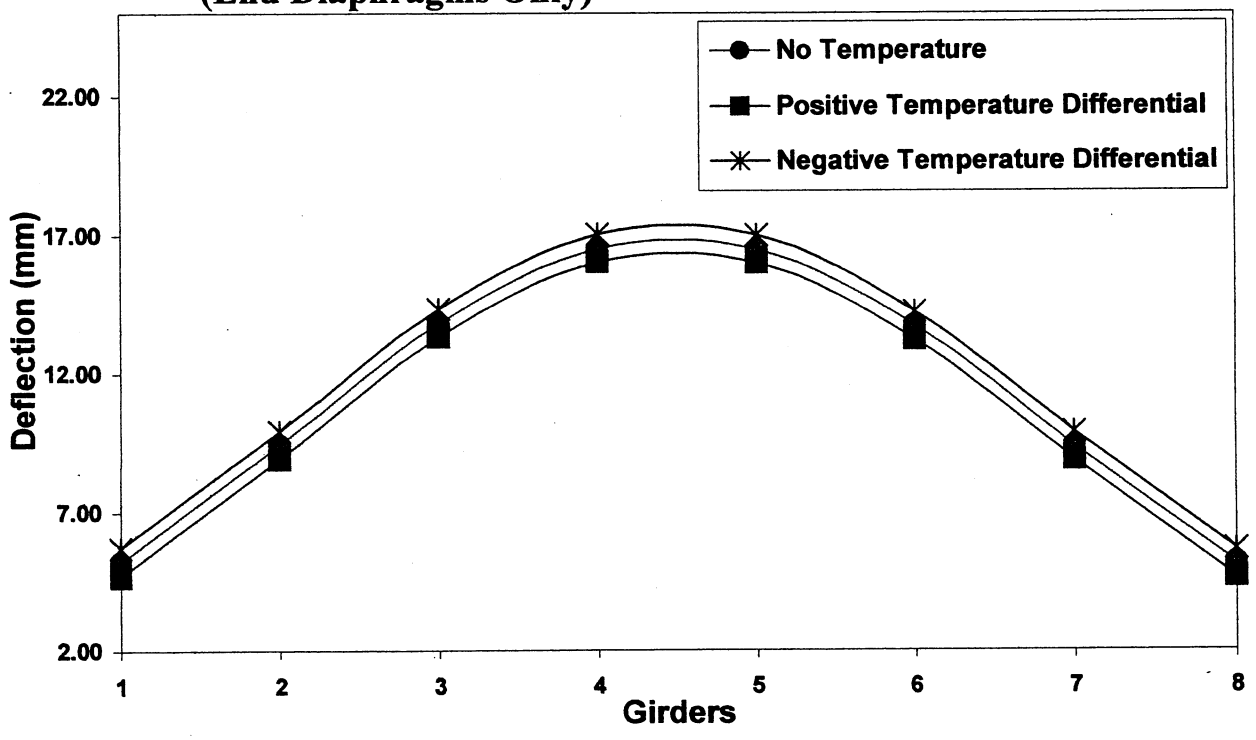

Figure 5.13 Comparison of Maximum Deflection, 15° Skew Angle with Temperature Differentials, G = 0.655 GPa (End Diaphragms Only)

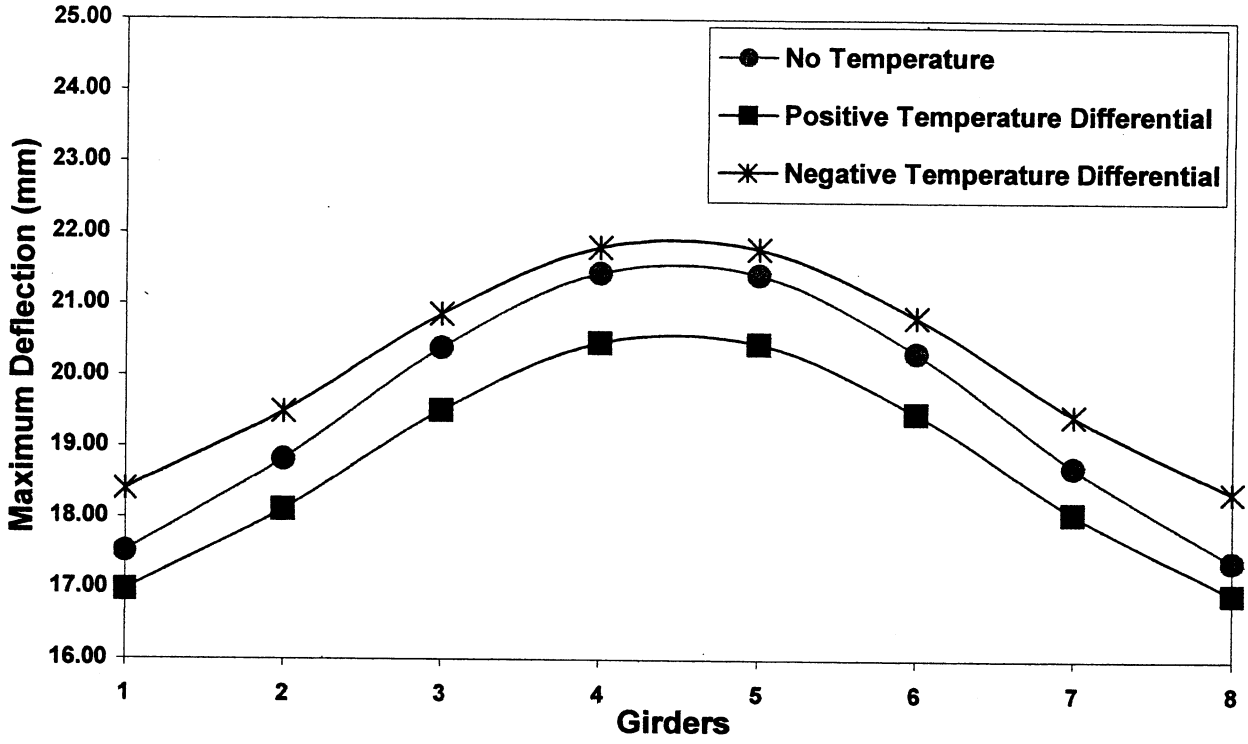

Figure 5.14 Comparison of Maximum Deflection, 60° Skew Angle with Temperature Differentials, G = 0.655 GPa (End Diaphragms Only)

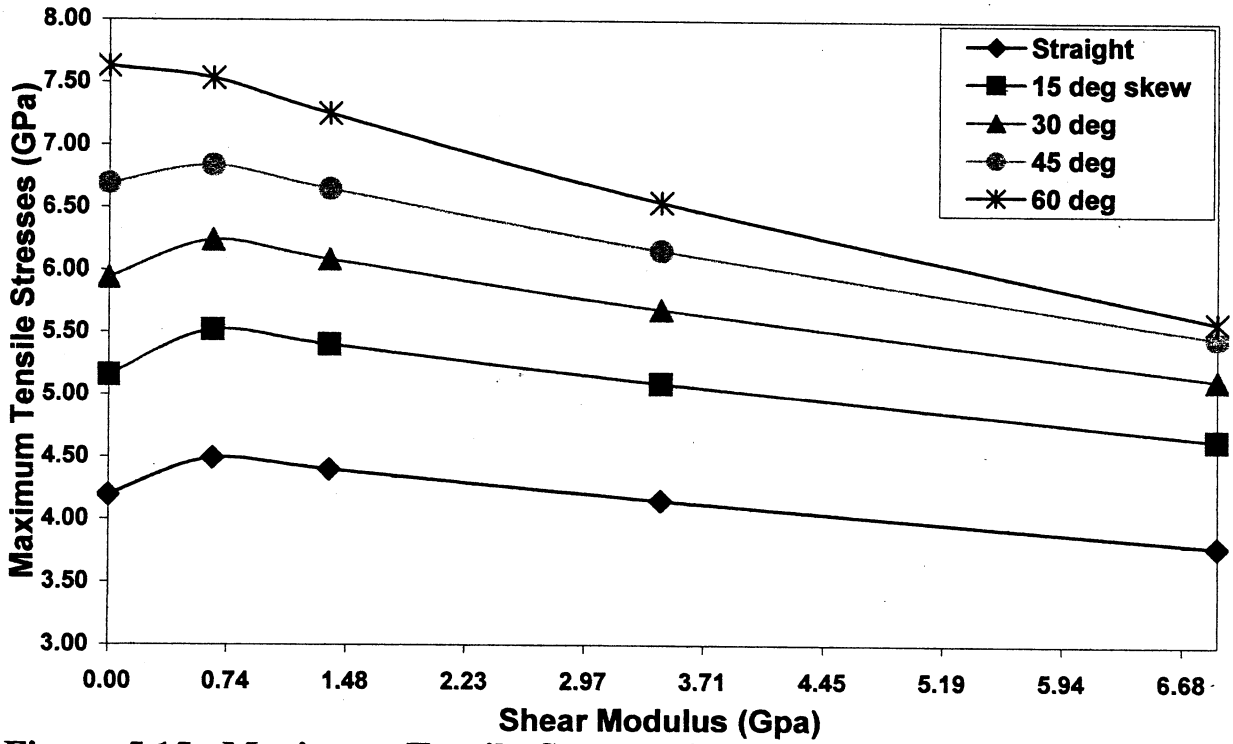

Figure 5.15 Maximum Tensile Stresses for Various Bearing Stiffness and Skew Angles, Positive Temperature Differential (End Diaphragms Only)

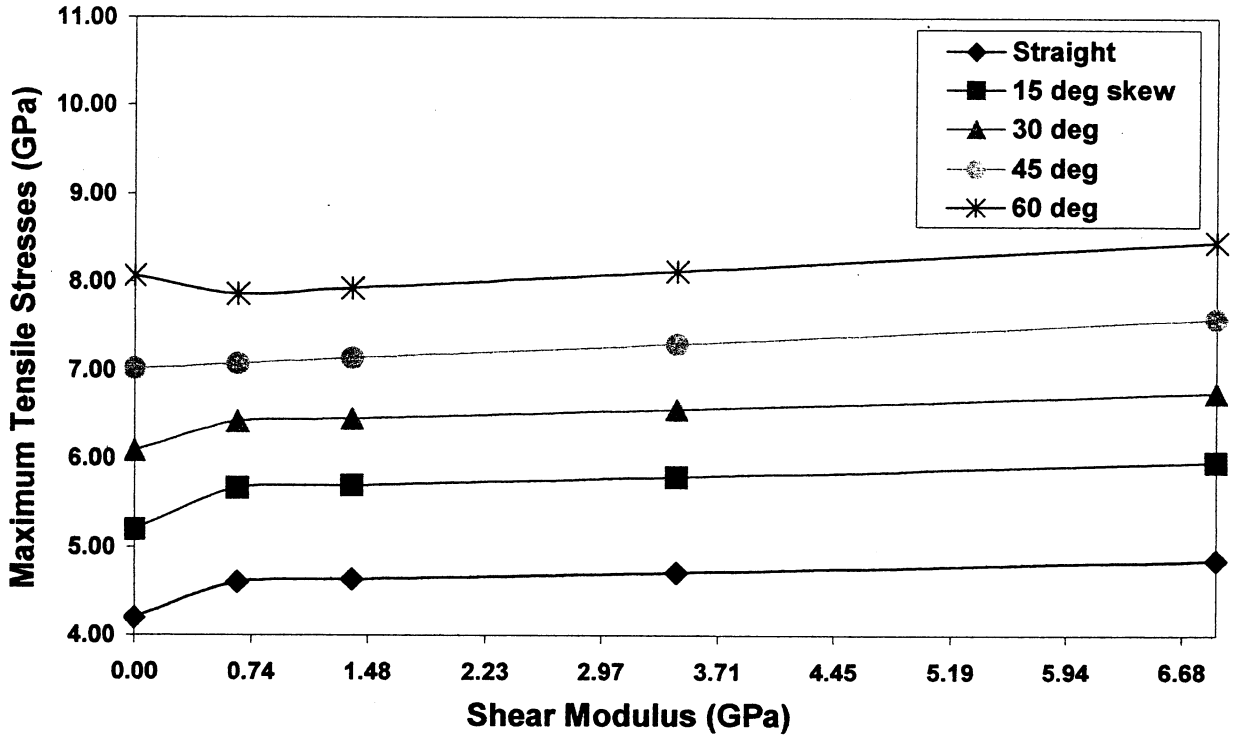

Figure 5.16 Maximum Tensile Stresses for Various Bearing Stiffness and Skew Angles for Negative Temperature Differential (End Diaphragms Only)

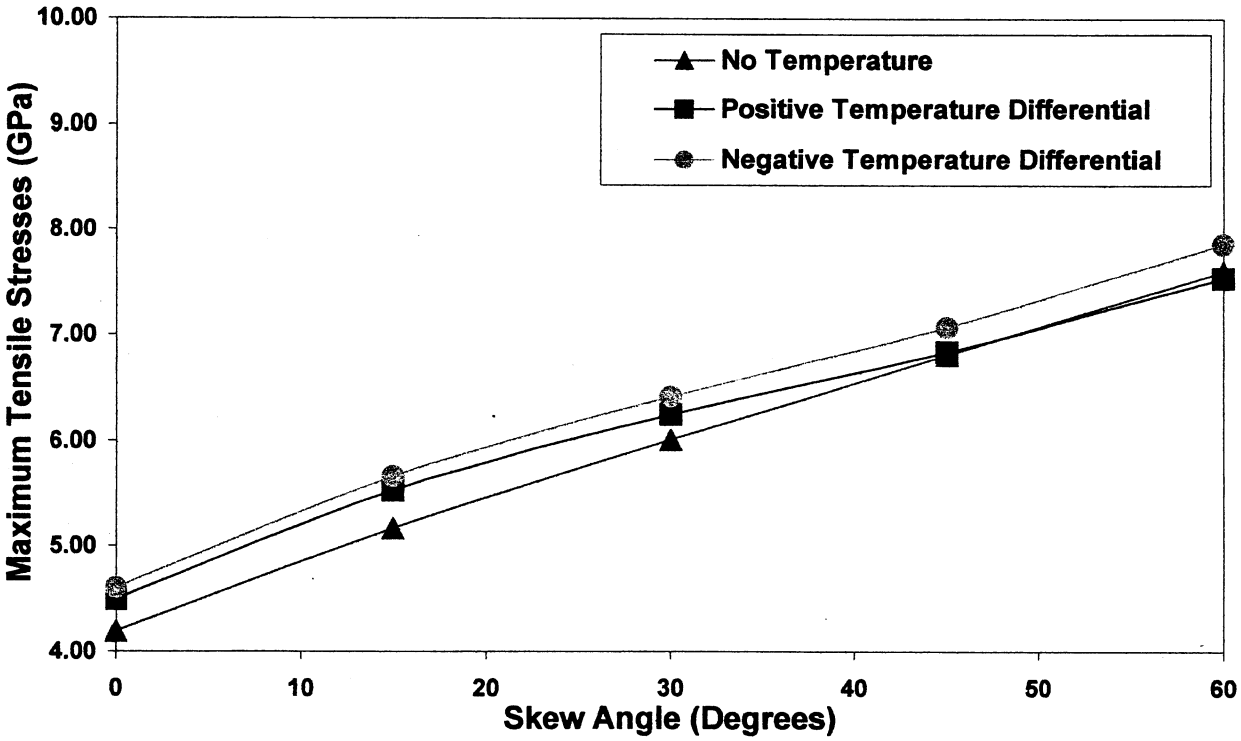

Figure 5.17 Comparison of Maximum Tensile Stresses for Various Skew Angles, and Temperature Differentials for G = 0.655 GPa (End Diaphragms Only)

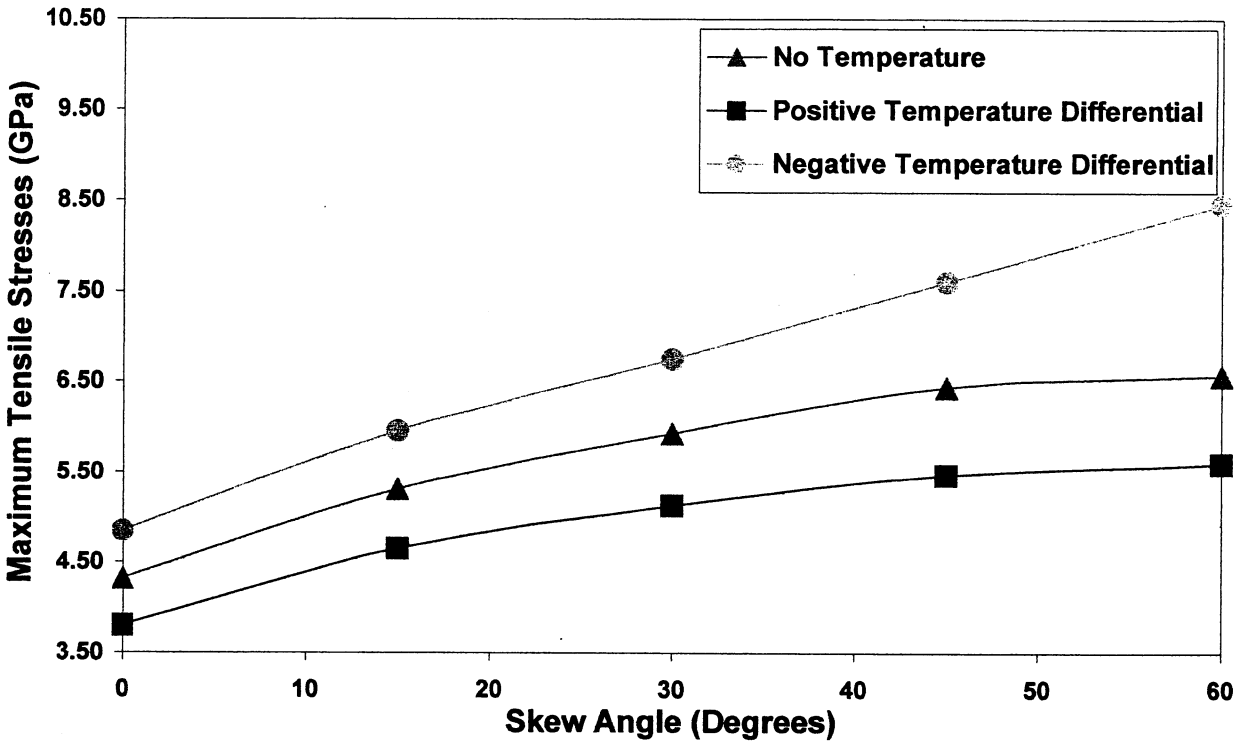

Figure 5.18 Comparison of Maximum Tensile Stresses for Various Skew Angles, and Temperature Differentials for G = 6.895 GPa (End Diaphragms Only)

5.4.1 Discussion

The results presented in Tables 5.21 and Fig. 5.11 are the deflection results due to a positive temperature differential load placed on the model. These results show that the expansion due to positive temperature changes is causing the deflection to increase as the skew angle increases and to decrease as the bearing stiffness increases, except for G=6.895 GPa case. This anomaly might be due to the combined effects of both a high stiffness and a large skew angle. This indicates that as the bearing stiffness increases, the horizontal reactions are causing a camber-like effect to counter the expansion. This would suggest that as the temperature increases, a higher bearing stiffness is beneficial to the girder. Table 5.22 and Fig. 5.12 present the results due to a negative temperature differential, with the contraction of the girder due to negative temperature changes. This contraction causes the maximum deflection of the girders to increase due to

increasing bearing stiffness and skew angle. Figures 5.13 and 5.14 compare the effect on the deflection due to temperature differentials for skewed models of 15° and 60°, respectively. Table 5.23 and Fig. 5.15 present the maximum tensile stresses of the girders as the shear modulus and skew angle increase for a positive temperature change. The results indicate that the midpoint stresses decrease as the bearing stiffness increases and increases with the skew angle. These results are consistent with the deflection results indicating an improved negative moment due to the reaction of the bearing pads. Table 5.24 and Fig. 5.16 present the results obtained for a negative temperature change. These results are consistent with the results obtained for deflection. As the deflection increases, increasing tensile stresses will appear in the bottom of the girder. These results also indicate that as the skew angle increases, the maximum tensile stresses increase due to negative temperature changes. This would indicate that the horizontal reactions from the bearing pads are acting outward due to the negative temperature change, adding to the positive load moments. This suggests that newer bearing pads with smaller stiffness are desirable rather than older, stiffer pads. Figures 5.17 and 5.18 compare the maximum tensile stresses at specified bearing stiffnesses as the skew angle increases.

CHAPTER 6

CONCLUSIONS AND RECOMMENDATIONS

The following conclusions may be made based upon the parametric analysis of currently specified FDOT type bearing pad specifications and theoretical modeling of the Florida Bulb Tee 78 precast concrete bridge girders.

1. Increasing the bearing stiffness has the overall benefit of reducing the midpoint deflections and tensile stresses of the bridge. However, during negative temperature changes this effect is reversed.
2. Skew angle of a bridge has a significant effect on bridge performance. Greater skew angle results in higher deflection and tensile stresses for the same pad stiffness. Higher skew angles need bearing pads with higher shear modulus to reduce midpoint deflection.
3. Lower skew angles may cause an uplift effect at the end girder supports, causing possible loss of contact with the bearing pads. This effect reduces as the skew angle increases. The uplift is generally confined to the external girders only.
4. Intermediate diaphragms have the effect of reducing the overall midpoint deflections and maximum stresses for the bridge system creating a beneficial reason for the application of the intermediate diaphragms. However, the reductions are smaller for increasing skew angles. Deflection may reduce by about 17% for straight bridges, but only about 5% for a 60° skew.

5. The application of the intermediate diaphragms has the added effect of eliminating the loss of girder contact with the bearing pads. This beneficial effect was apparent for all stiffnesses and skew angles.

6. The expansion of the bridge due to a positive temperature change decreases midpoint deflections and tensile stresses as a result of the bearing pad effects. As the bearing stiffness increases, a camber-like effect occurs providing a beneficial effect on the bridge system.

7. The contraction of the bridge due to a negative temperature change has the effect of increasing the midpoint deflection and tensile stresses when using bearing pads. Due to the combined loads of live load as well as temperature loads, the results indicate that as the temperature decreases, the shear modulus of the bearing pad should be reduced to reduce midpoint deflections.

Based on this study it is recommended that ordinary bearing pads provide adequate horizontal movement with minimal restraining forces applied to the girder. The effect of increasing the bearing stiffness has been shown to be both beneficial and detrimental to the bridge system depending on the conditions. Laminated neoprene bearing pads provide an economic girder support system. It is recommended that a more extensive study be conducted on the effects of end and intermediate diaphragms placed on the bridge.

BIBLIOGRAPHY

1. Aldridge, Weldon W., Sestak, Joe J., and Fears, Fulton K., "Tests on Five Elastomeric Bridge Bearing Materials", *Highway Research Record,* Number 253, 1968.

2. American Association of State Highway and Transportation Officials (AASHTO), "Standard Specifications for Highway Bridges – Load and Resistance Factor Design", Washington, D.C., 1999.

3. ANSYS Elements Manual, SAS IP, 1999.

4. Arockiasamy, M., Amer, Ahmed, and Bell, Nathaniel B., "Load Distribution on Highway Bridges Based on Field Test Data: Phase II", Final Report Submitted to the Florida Department of Transportation, Tallahassee, July 1997.

5. Bakht, Baider, "Observed Behavior of a New Medium Span-on-Girder Bridge", Structural Research Report SRR-88-02, Ministry of Transportation, Ontario, June 1988.

6. Bakht,, Baider and Jaeger, Leslie, "Bearing Restraint in Slab-on-Girder Bridges", *Journal of Structural Engineering*, v 114, n 12, December 1988.

7. Bakht, Baider and Jaeger, Leslie, "Ultimate Load Test of Slab-on-Girder Bridge", *Journal of Structural Engineering,* v 118, n 6, June 1992.

8. Bishara, Alfred G., Liu, Maria Chuan, and El-Ali, Nasser D., "Wheel Load Distribution on simply supported skew I-beam composite bridges", *Journal of Structural Engineering*, v 119, n 2, February 1993.

9. Brielmaier, A. A., "Neoprene bridge pads: fatigue behavior in compression and shear", Pennsylvania State University, College of Engineering, 1964.

10. Clark, Earl V. and Moultrop, Kendall, "Load-Deformation Characteristics of Elastomeric Bridge Bearing Pads", *Highway Research Record*, Number 34, 1963.

11. DuPont, Engineering Properties of Neoprene Bridge Bearings, 1983.

12. Florida Department of Transportation (FDOT), "Structural Standards" Structures Design Office, Tallahassee, FL 1998.

13. Gent, Alan N., "Engineering with Rubber, How to Design Rubber Components", Hanser, New York, Oxford Univ. Press, 1992.

14. Gere, James M. and Timoshenko, Stephen P., "Mechanics of Materials" 4th Ed., PWS, Boston, 1997.

15. Eddy, Scott, "Effects of Elastomeric Bearing Pads on Highway Bridge Girders", MSCE Thesis Submitted to the Department of Civil Engineering, Florida State University, Tallahassee, FL, April 1998.

16. Khaleel, Mohammad A., and Itani, Rafik Y., "Live-Load Moments for Continuous Skew Bridges", *Journal of Structural Engineering*, v 116, n 9, September 1990, p 2360-2373.

17. Moorty, Shashi, and Roeder, C.W., "Temperature Dependent Bridge Movements", *Journal of Structural Engineering*, v 118, n 4, April 1992, p 1090-1105.

18. Nachtrab, William B. and Davidson, Robert L., "Behavior of Elastomeric Bearing Pads under Simultaneous Compression and Shear Loads", Pennsylvania Department of Highways, 1962.

19. Nawy, Edward G., "Reinforced Concrete: A Fundamental Approach", 3rd Ed., Prentice-Hall, Inc., 1995.

20. Nizamud-doulah, Shaikh Md., "Nonlinear Analysis of Reinforced Concrete Skew Slabs", MSCE Thesis Submitted to the Department of Civil Engineering, Bangladesh University of Engineering and Technology, Dhaka, India, July 2000.

21. Nordlin, E. F., Crozier, W. F., Stoker, J.R., Martin, V.C., "Laboratory Evaluation of Full-Size Elastomeric Bridge Bearing Pads",*Transportation Research Board Transportation Research Record,* n 547, 1972.

22. Roeder, C.W., Stanton, J.F., and Feller, T., "Low Temperature Behavior and Acceptance Criteria for Elastomeric Bridge Bearings", *National Cooperative Highway Research Program*, Report 325, 1989.

23. Roeder, Charles W., Stanton, John F., and Feller, Troy, "Low Temperature Performance of Elastomeric Bearings", *Journal of Cold Regions Engineering,* v 4, n 3, September 1990, p 113-132.

24. Stanton, John F. and Roeder, Charles W., "Elastomeric Bearings, An Overview", *Concrete International*, v 14, n 1, January 1992, pp. 41-46.